

# Wireless Implantable Microsystems: High-Density Electronic Interfaces to the Nervous System

K. D. WISE, FELLOW, IEEE, D. J. ANDERSON, J. F. HETKE, D. R. KIPKE, MEMBER, IEEE, AND K. NAJAFI, FELLOW, IEEE

## Invited Paper

*This paper describes the development of a high-density electronic interface to the central nervous system. Silicon micromachined electrode arrays now permit the long-term monitoring of neural activity in vivo as well as the insertion of electronic signals into neural networks at the cellular level. Efforts to understand and engineer the biology of the implant/tissue interface are also underway. These electrode arrays are facilitating significant advances in our understanding of the nervous system, and merged with on-chip circuitry, signal processing, microfluidics, and wireless interfaces, they are forming the basis for a family of neural prostheses for the possible treatment of disorders such as blindness, deafness, paralysis, severe epilepsy, and Parkinson's disease.*

**Keywords**—Microelectrodes, microfluidics, micromachining, microsystems, nervous system, neural implants, sensors.

## I. INTRODUCTION

Man has struggled to understand the nervous system and develop treatments for its disorders for centuries. Benjamin Franklin explored the use of electrical currents as an approach to overcoming paralysis [1], but it was not until the last century that investigations at the cellular level were really possible. Today, both our understanding of the nervous system and our ability to treat a variety of its disorders using neural prostheses appear ready to make dramatic progress as the result of combining bioMEMS with microelectronics.

Manuscript received March 23, 2003; revised July 28, 2003. This work was supported in part by the Neural Prosthesis Program of the National Institute of Neurological Disorders and Stroke, National Institutes of Health (NIH), in part by the NIH National Center for Research Resources, in part by the National Institute of Biomedical Imaging and Bioengineering, and in part by the Engineering Research Centers Program, National Science Foundation under Award EEC-9986866.

The authors are with the Engineering Research Center for Wireless Integrated MicroSystems, University of Michigan, Ann Arbor, MI 48109-2122 USA.

Digital Object Identifier 10.1109/JPROC.2003.820544

Beginning in the 1950s, the use of microelectrodes together with electronic recording and signal processing began to allow meaningful studies of the central nervous system at the cellular level [2]. Gradually, a great deal was learned about the workings of single neurons. Serially moving sharpened wire electrodes in tissue also allowed considerable information to be gained about the function of the nervous system at the circuit level, especially in sensory areas. However, it was quickly clear that arrays of electrodes, and perhaps large arrays, would be needed to really understand the signal processing performed in complex neural networks. Early experiments facilitated by gluing individual electrodes together or using cutoff wire bundles [3], [4] to record simultaneously from many points met with some success but were limited in their geometries and reproducibility, caused considerable insertion damage, and tended to splay out in tissue, making exact site placements uncertain. Nevertheless, they could be fabricated easily with available technology. Microwire electrode arrays are still used extensively for both acute and chronic extracellular recording [5]–[7].

In 1965, Prof. J. L. Moll at Stanford University, Stanford, CA, suggested that the lithographic techniques and silicon etching technology then being developed for beam-lead integrated circuits (ICs) [8] at Bell Telephone Laboratories might be used to produce electrode arrays capable of recording from many points in tissue simultaneously and with no more damage than a single metal microelectrode. Professor J. B. Angell led a project that soon demonstrated such electrodes [9]–[11]; however, at this point, the technologies available for silicon etching were not sufficiently precise to allow the probes to be produced reproducibly with high yield. The needed technology was developed over the next two decades as part of the more general development of integrated sensors and microelectromechanical systems (MEMS). During

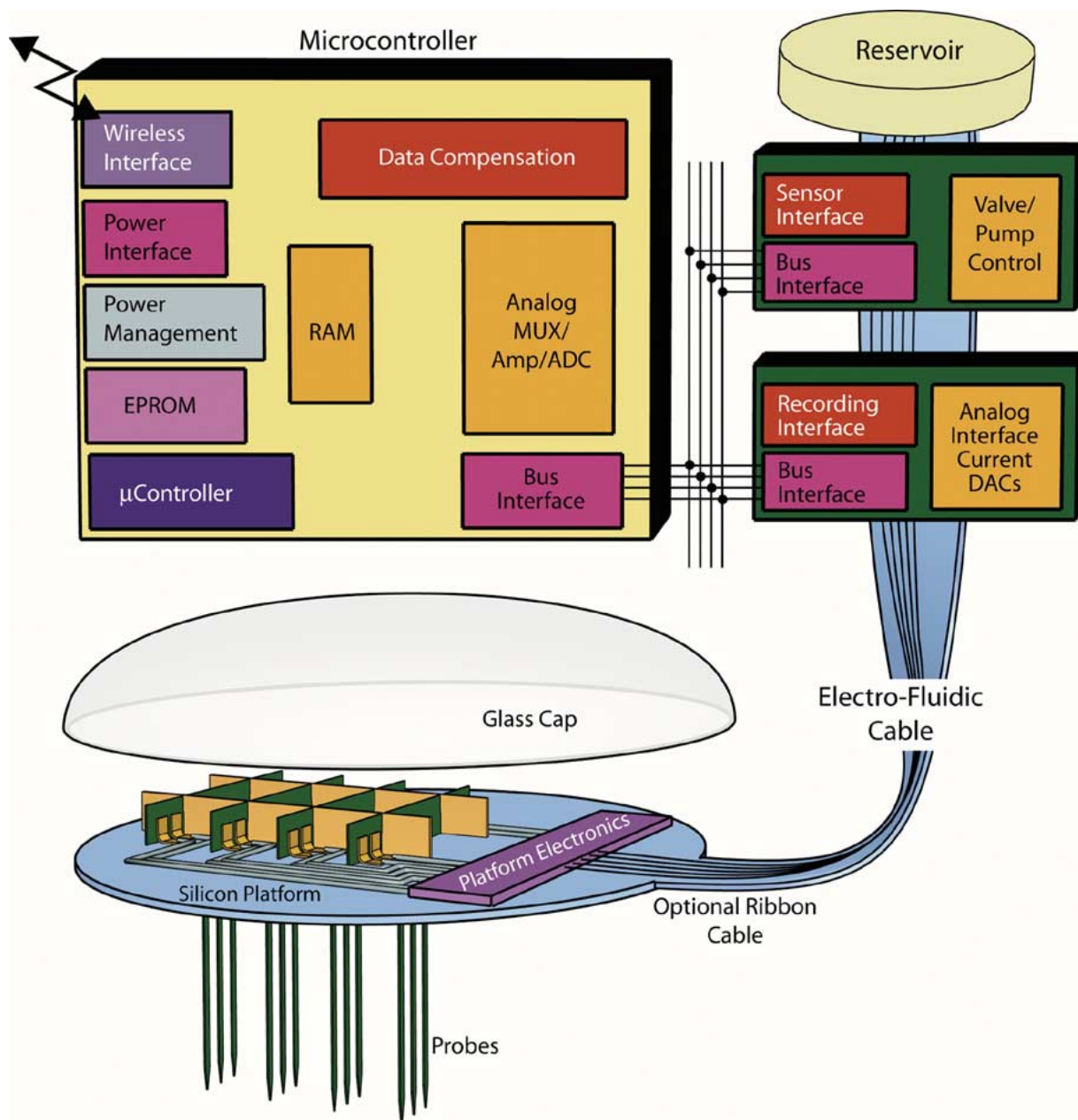


**Fig. 1.** Diagram of a generic neural prosthesis and electronic interface to the nervous system. For applications not requiring drug delivery, all electronics could be on the platform, eliminating the implanted cable.

the past decade, the resulting probes have begun to change research directions in the neurosciences.

Work to develop implantable prosthetic devices for the deaf and the blind also began in the 1960s using arrays of metal electrodes implanted in the cochlea [12], auditory nerve [13], inferior colliculus [14], and visual cortex [15]. Electrode placement was difficult in these early experiments and all electronics was external, but over time, information on appropriate stimulus parameters and physiological responses was obtained. Full systems sufficient to realistically assess the performance of an eventual prosthesis were not possible, however. In many cases, problems with the electrodes, leads, packaging, and the electronics were severe, even for short-term animal experiments, and the systems

realized fell far short of those required for human use. Gradually, we have moved forward in our understanding of relevant physiology and in the hardware required for a practical assessment of the efficacy of such devices. Today, neural prostheses are emerging to work real miracles in helping people, and far greater progress is likely in the decade to come. Over 70 000 cochlear prostheses have been implanted worldwide to date, and with them the profoundly deaf can often hear well enough to use the telephone and interact normally in a hearing world [16]. During the coming decade, many, and perhaps most, cases of profound deafness may be reduced to treatable disorders. Retinal implants have recently received great attention [17], [18], and many efforts to develop them are underway worldwide.

Deep-brain electrodes for managing severe Parkinson's disease have proven remarkably effective [19], even though the mechanisms by which they operate are not yet completely understood. Devices for managing severe epilepsy are in development, and the first experiments aimed at capturing motor control signals from the cortex to eventually restore at least limited movement to quadriplegics have been promising [20]–[22].

All of these efforts to better understand the nervous system and develop practical prostheses for its disorders depend on building an electronic (and perhaps chemical) interface to the cellular world. Fig. 1 shows one possible form for such an interface, where a high-density three-dimensional (3-D) electrode array penetrates the tissue to monitor its electrical activity (record), insert electrical signals (stimulate), or control the local chemical environment (drug delivery). The individual probe shanks supporting the recording, stimulating, and drug delivery sites should be small enough to be virtually invisible to the tissue. The interface electronics is partitioned here between the probes themselves, the platform, and in some cases, a remote electronics package. Excluding the need for any chemical reservoir, the structure could be self-contained, remotely powered, monitored, and controlled using a bidirectional RF telemetry link. While this system could take a number of physical forms, it is envisioned here as a button-size implant with a diameter of a few millimeters and a height above the platform of no more than 1 mm. The key parts of any such system are the electrodes themselves, the interface electronics, the wireless link, and the packaging. This paper describes recent progress in each of these areas.

## II. SILICON MICROMACHINED ELECTRODE ARRAYS

Traditional metal microelectrodes [23]–[25] are electrolytically sharpened wires (pins), 25 to 50  $\mu\text{m}$  in diameter and insulated to define an exposed recording area at the tip of perhaps 100  $\mu\text{m}^2$ . Such electrodes record the local voltage associated with ionic current flow around a neuron when it fires in response to inputs received from other cells. The electrode sites are capacitive with an impedance of a few megohms at 1 kHz. Recorded signals range from the noise level [2] (20  $\mu\text{V}$  or so) to about 1 mV, with an extracellular signal bandwidth of perhaps 10 kHz. In contrast, KCl-filled glass micropipettes [26] allow penetration of the cell membrane and result in signals of several tens of millivolts but are generally useful only for intracellular studies. Their recording bandwidths are limited due to capacitive loading of their high tip resistances. In contrast to these discrete approaches, the structure of a typical thin-film probe is shown in Fig. 2. Here, all dimensions are lithographically controlled to better than 1  $\mu\text{m}$ . An array of recording/stimulating sites is connected to circuitry at the rear of the structure via thin-film conductors that are insulated above and below by deposited dielectrics. The most critical aspects of these probes are the substrate and how it is shaped, the sites, the interconnects and their encapsulation, and the interface to signal processing electronics. Such probes have been in development since 1966, with many variations in the structures and materials used.

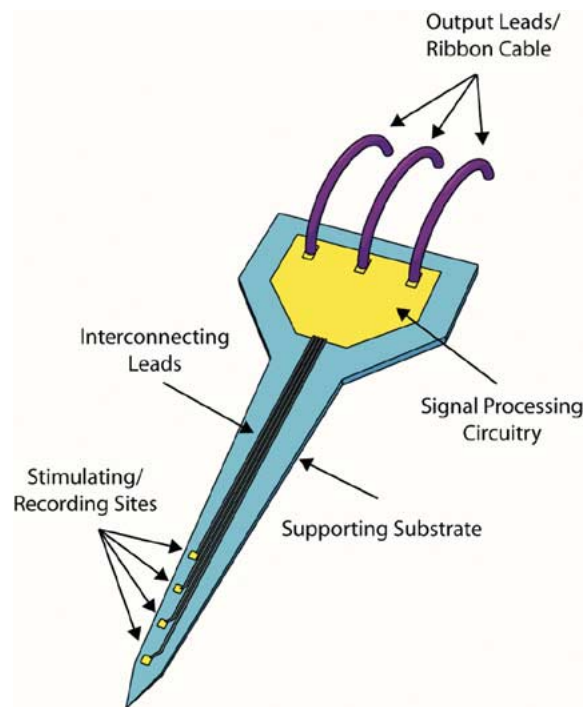
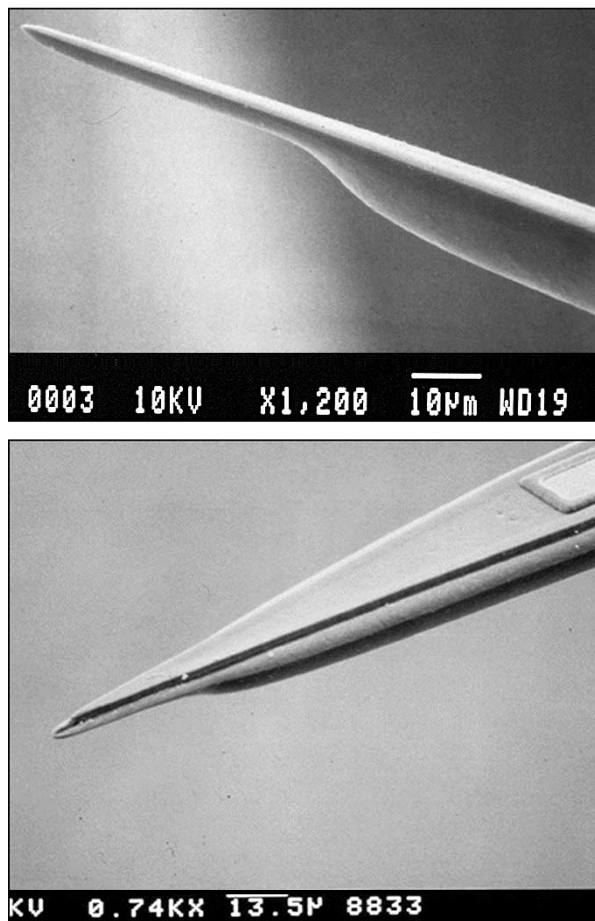


Fig. 2. Diagram of a silicon micromachined neural probe.

### A. The Probe Substrate

The probe substrate is arguably the most important part of the entire structure. It must be biocompatible, small enough to avoid traumatizing the tissue, and, ideally, strong enough to penetrate the pia arachnoid membrane over the brain. Many substrate materials were explored in the early days of probe development, including silicon [11], [27], sapphire [28], glass [29], metal foils [30], [31], and polymers [32]. These efforts generally met with only limited success. In some cases, recordings were reported using the resulting probes, but fabrication was often so challenging that projects did not go beyond a few initial prototypes. Although recording single units acutely over minutes to hours can be accomplished with many structures, the goal of a chronic tissue interface that is stable over many years *in vivo* is a far more challenging problem.

Silicon has well-recognized advantages in probe fabrication. It allows use of the well-established technologies and equipment developed for the semiconductor industry, and today can be shaped with a precision greater than perhaps any other material [33]. Isotropic silicon etchants were joined by anisotropic etchants and impurity-based boron etch-stops in the 1970s and by deep reactive-ion etching (DRIE) in the 1990s. Boron etch-stops permit the silicon substrate to be defined by a deep boron diffusion (typically, a 6–7 h open-tube solid-source predeposition step at 1175  $^{\circ}\text{C}$ , followed by a comparable drive-in). A second (shallower) diffusion, can be used to taper the tip if desired, as shown in Fig. 3. The diffusion rounds the edges of the probe, producing a smooth taper to a sharp tip. The importance of such features have not been quantified but may be significant in pushing the tissue out of the way instead of cutting during insertion. Silicon is slowly



**Fig. 3.** Scanning electron microscopy side view of a silicon probe substrate defined using a shallow (tip) and deep (shank) boron etch-stop (above) and perspective view (below).

attacked in saline; however, the use of a boron etch-stop to define the substrate virtually eliminates such erosion [34]. The shunt capacitance added by the conducting substrate is typically negligible compared to the site impedance, especially as conductor widths decrease, while the heavy substrate doping minimizes electrically or optically induced noise and virtually eliminates interelectrode crosstalk [35]. The substrate acts as a ground plane under the interconnects, while the extracellular fluid acts as a ground plane above them. Finally, the use of silicon allows integrated electronics to be formed directly in the probe substrate, eliminating the many lead transfers that would otherwise be required.

The thickness of the silicon substrate can be varied by controlling the boron diffusion used to define it, from a few tenths of a micrometer [36] to 15  $\mu\text{m}$  or more, and using a dry substrate etch (DRIE) to limit substrate spreading due to lateral diffusion, substrates as narrow as 5  $\mu\text{m}$  have been realized. Shank width is limited not by technology but by strength [37]. It is important that the implant float in the brain, independent of the skull, in order to minimize any movement relative to the tissue and resulting tissue reaction. Today, boron-etch-stopped silicon substrates are widely used and, combined with DRIE, allow the integration of ribbon cables and signal processing electronics into the probe substrate as described below. Other silicon probe processes have

also been demonstrated [38]–[41] based on dry etching and silicon-on-insulator (SOI) technologies. Each of these has its own unique set of advantages and limitations.

### B. Probe Interconnects and Their Encapsulation

Thin-film leads must connect the exposed metal recording/stimulating sites on the probe to any on-chip electronics or output pads. For recording probes, lead resistance is not particularly important, and even polysilicon (10  $\Omega/\text{square}$ ) has been adequate. However, as shank widths are scaled down and the number of sites is increased, it will become increasingly important to reduce the resistance of the interconnect material further. The seal that this material makes with the dielectric used to insulate it is of critical importance. Even though silicon dioxide is known to hydrate slowly in water, compound inorganic dielectric stacks of silicon dioxide and silicon nitride have performed well *in vivo* when deposited by low-pressure chemical vapor deposition (LPCVD). The layer thicknesses in such stacks are ratioed so that any stress in the overall film is near neutral and the probe does not warp. These materials are well known in the semiconductor industry and can be deposited from about 400  $^{\circ}\text{C}$  [plasma-enhanced CVD (PECVD) or low-temperature oxide (LTO)] to 800–900  $^{\circ}\text{C}$  (LPCVD films). The LPCVD dielectrics are higher in quality and less prone to pinholes but place obvious constraints on the metals over which they can be applied, especially since they must be rather thick (1–1.2  $\mu\text{m}$ ). The advantage of polysilicon is that it forms an intimate junction with silicon dioxide, eliminating any risk of separation or fluid encroachment around the sites. Leads formed from polysilicon with LPCVD oxide/nitride/oxide dielectrics have produced stable impedances *in vivo* for more than a year. Their performance over decades, consistent with prosthetic applications, is still unknown, and additional dielectric overcoats such as diamond are being explored. For lower interconnect sheet resistances, refractory metals and their silicides are being investigated. For example, titanium silicide is compatible with LPCVD dielectrics and produces sheet resistances of 1–2  $\Omega/\text{square}$ , adequate for most stimulating electrodes and some cables. Fig. 4 summarizes the basic process flow for a probe without on-chip circuitry, while Fig. 5 shows a typical multishank probe.

Without telemetry, communication between the implanted probe and the outside world must be achieved through a multichannel interconnect cable and a percutaneous connector, and even when telemetry is used, a cable may be necessary to link the probes to a telemetry platform as noted in Fig. 1. The electrical, mechanical, and chemical stability of this link is critical to the overall success of the implant since, as noted above, it must minimize tethering and permit the probe to float freely in the brain. Its size should be on the same scale as the probe to which it is attached and yet it must be mechanically robust in order to withstand surgical manipulation, the rigors of healing, and in some cases tunneling through skin and muscle. As with the probe, the cable and its attachment to the probe must be electrically stable and biocompatible.



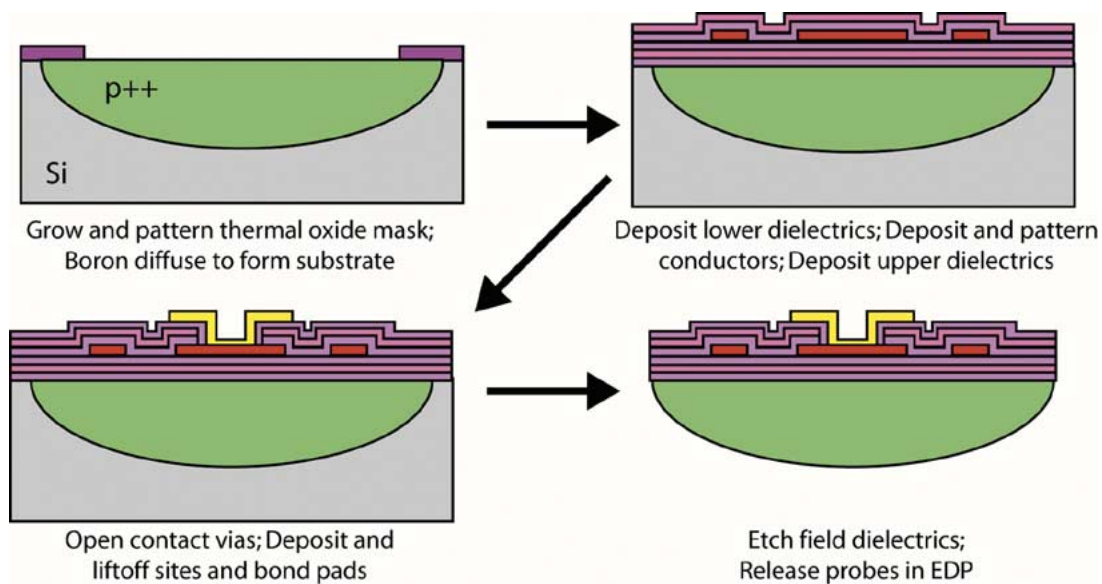


**Fig. 4.** Basic process flow for a passive silicon micromachined electrode array.

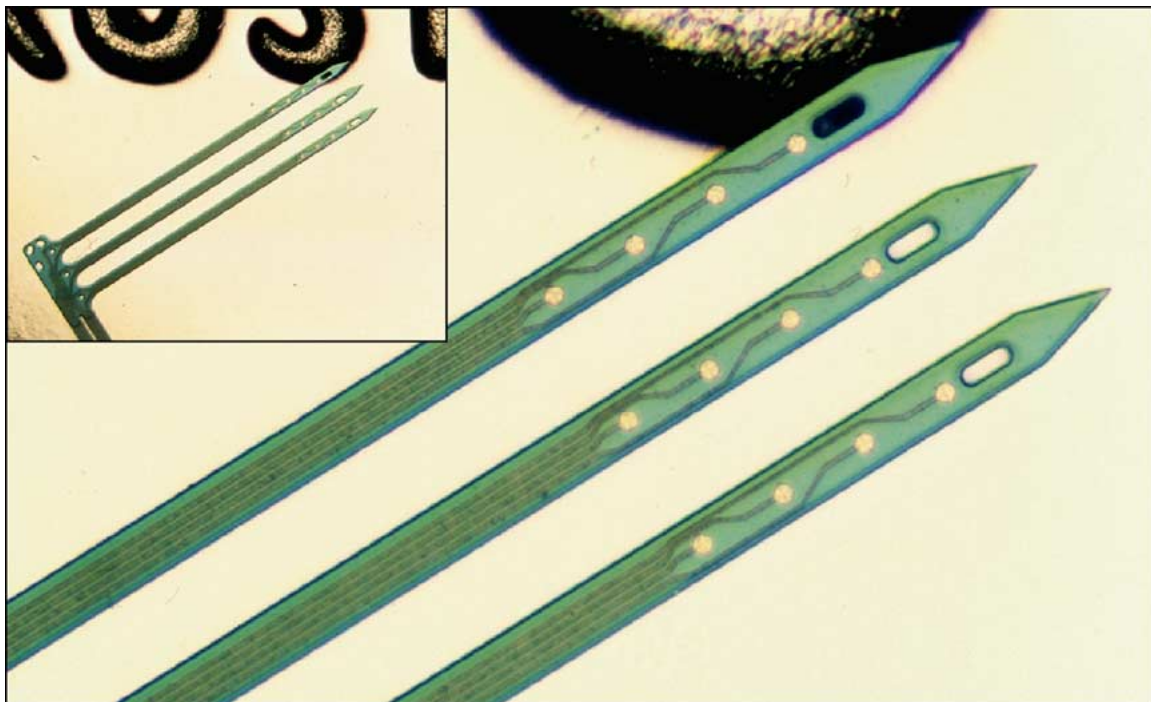


**Fig. 5.** Picture of a three-shank 12-site recording probe. Holes in the shanks may help stabilize the probe in tissue in chronic recording situations. The probe is next to the “TRUST” on a U.S. penny.

Early attempts to solve this off-chip lead problem, and some more recent ones [42], have utilized multiple discrete wire leads fashioned after the wire electrodes used by Schmidt *et al.* [43]. This technique involves soldering or gluing with conductive epoxy individually insulated wires to each pad on the electrode, a labor-intensive process that requires substantial area to accommodate large bonding pads on the back of the probe. When more than a few wires are used, the resulting cable becomes quite bulky and relatively rigid. Microfabricated cables are an obvious alternative to discrete wires, and several types have been explored.

Silicon-based ribbon cables [44] were the first step in the realization of a successful chronic implant with the “Michigan probes.” These cables, shown in Fig. 6, can be monolithically integrated with the probes themselves and use a shallow boron diffusion to define the cable substrate. This results in a cable that has an overall thickness of about 4  $\mu\text{m}$  and is extremely flexible; even with multiple leads, a silicon cable is roughly 100 times more flexible than a single 25- $\mu\text{m}$ -diameter gold wire and requires no connections to be made with the probe [37]. Soak tests performed on the LPCVD dielectrics used on the probes and cables indicate that the structures will

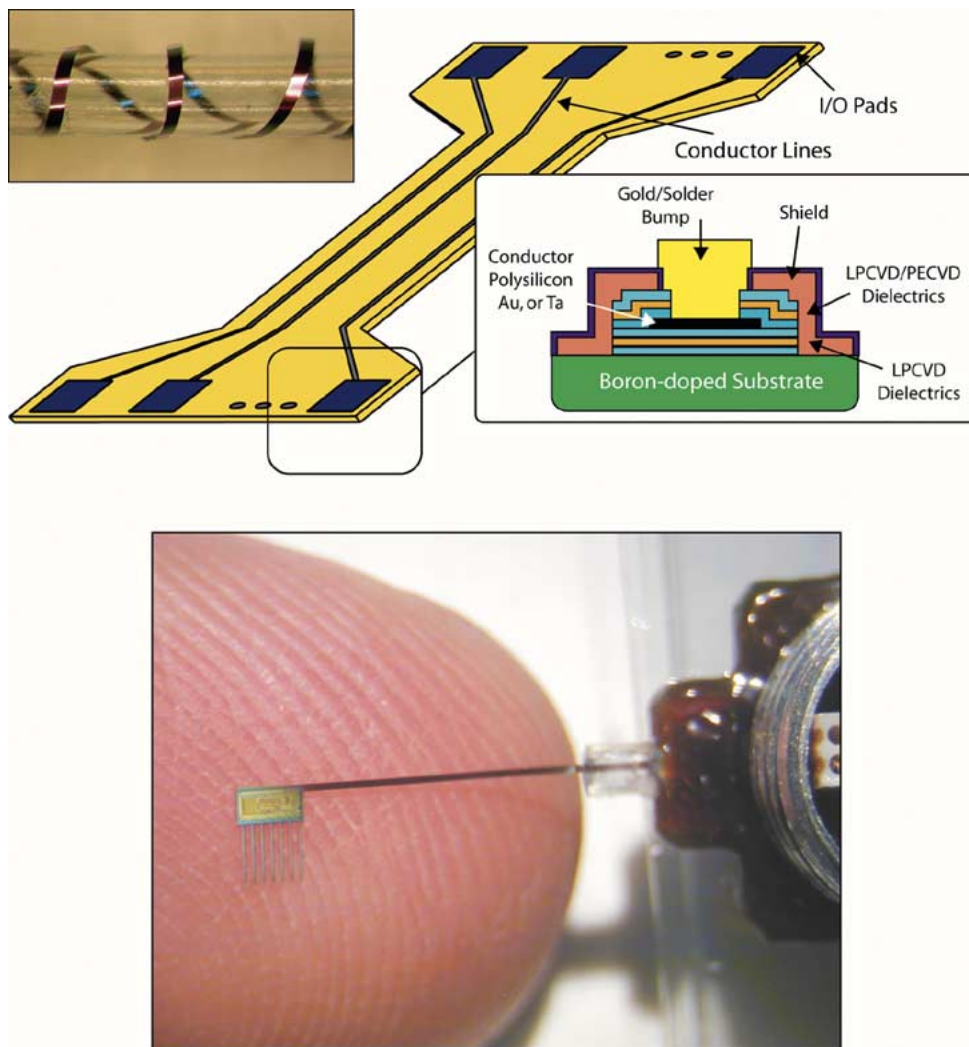


**Fig. 6.** Top: silicon ribbon cable (with inset showing a cable wrapped around a 1-mm-diameter glass rod). Bottom: multichannel probe with integrated ribbon cable.

maintain subpicoamp leakage currents for at least four years *in vitro* [44]. Sixteen-channel cables with widths of  $200\ \mu\text{m}$  and lengths of 1 cm have recorded unit data for periods exceeding one year in rats [45].

While thin silicon is very flexible out-of-plane, in-plane bending, stretching, and radical twisting can cause it to break. Furthermore, lengths longer than a few centimeters are not practical due to high aspect ratios that significantly lower yield. Therefore, for implant situations requiring longer and more robust connections, silicon cables will need to be teamed with a stronger secondary polymer cable. A variety of polymers are being investigated, including polyimide [46]–[49].

### C. Recording and Stimulating Sites

Sensing of the biopotentials generated by active neurons is done using exposed metal sites. To avoid potential averaging, the site should be small relative to the total spatial potential spread in tissue ( $30\text{--}100\ \mu\text{m}$ ) [50], but making sites very small increases their impedance levels and thermal noise. Typical site dimensions today are from 6 to perhaps  $20\ \mu\text{m}$  for recording, with corresponding geometrical areas from 40

to  $400\ \mu\text{m}^2$ . For stimulation, the minimum site area is limited by the required charge delivery, and this can be a significant problem, especially for prosthetic applications. Cell thresholds depend on how closely the site approaches the cell and vary from about  $10\ \mu\text{A}$  (3 nC) in cortex and cochlear nucleus to perhaps  $300\ \mu\text{A}$  (12 nC) in the cochlea and retina. The ability to couple high charge densities into tissue is critically important, and small sites produce high back-voltages in tissue due to the spreading resistance near the site. The use of waffled sites can help this situation by maximizing the effective site periphery [51].

Gold, platinum, and iridium (iridium oxide) have all been used for stimulating sites. Gold has a maximum charge delivery of about  $20\ \mu\text{C}/\text{cm}^2$ , whereas platinum can deliver up to  $75\ \mu\text{C}/\text{cm}^2$  and iridium oxide delivers as much as  $3000\ \mu\text{C}/\text{cm}^2$ , making it the material of choice for microstimulation [52]–[55]. Charge, and not current, stimulates cellular activity, and when driving the electrode, it is essential to remain within the “water window” to avoid evolving oxygen or hydrogen or inducing local pH changes. Charge-balanced biphasic pulses are used with typical pulse durations between 20 and  $500\ \mu\text{sec}$ , depending on the application.

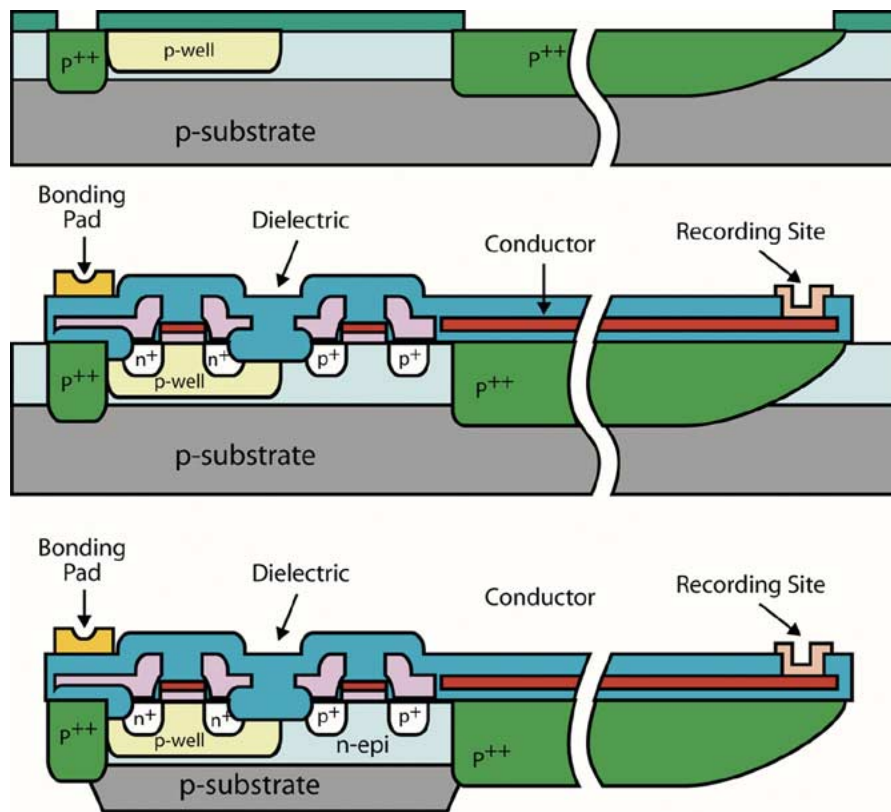


**Fig. 7.** Fabrication of probes containing on-chip CMOS circuitry: etch-stop and p-well formation; circuit fabrication and encapsulation; release from the wafer.

Iridium oxide is a multilayered film that undergoes charge injection valence changes in its oxidation state. Such films can be produced by reactively sputtering in oxygen [56], [57], electroplating [58], or, more typically, using anodization [59], [60]. Using the anodization process, the electrode is immersed in dilute sulfuric acid, carbonate-buffered saline (CBS), or phosphate-buffered saline (PBS) [54], [61], [62]. A triangular voltage is forced between the working electrode and a saturated calomel electrode (SCE) reference and is cycled between limits set by hydrogen and oxygen evolution. A hydrous oxide film builds in thickness on the iridium surface as the potential is continuously cycled. The hydrous oxide is very porous, allowing water to be absorbed into it and effectively increasing the surface area across which ions can be transferred.

Iridium oxide can attain charge capacities in excess of  $400 \text{ mC/cm}^2$  if the activation time is sufficiently long; however, surface cracks begin to appear in the film beyond about  $250 \text{ mC/cm}^2$  due to the stresses induced by volumetric expansion of the growing oxide. The amount of charge the film can actually deliver to solution is only a fraction of the total capacity [61], [62], increasing with charge capacity up to an activation of about  $100 \text{ mC/cm}^2$  and then plateauing at about  $1\text{--}3 \text{ mC/cm}^2$ .

#### D. On-Chip Circuit Fabrication

External leads are perhaps the most difficult problem associated with implanted electrode arrays, and on-chip circuitry is needed to decrease their number and increase the

amplitudes of the recorded neural signals. Both hybrid and monolithic circuit options are available on a silicon-substrate probe, with the latter eliminating the problems associated with lead transfers to hybrid circuitry at the expense of a more complex fabrication process.

The cross section of an active neural probe is shown in Fig. 7. The circuitry here is fabricated in an n-epitaxial region on a p-type substrate. This allows the electronics to be completely surrounded by a grounded p-layer, which contacts the tissue and yet allows both positive and negative voltages to be used in the circuitry. The process begins with deep and shallow diffusions to define the intended substrate. Stress-compensated dielectrics are deposited, the p-well is implanted, and the p-well drive-in is performed along with the last portion of the etch-stop diffusions [Fig. 7 (top)] [63]. A standard p-well CMOS process is then used to form the circuitry, described below. Contacts are opened and formed using titanium and titanium nitride plugs with stacked aluminum and titanium metallization [63], [64]. Thick plugs are required to prevent spiking during the deposition of a low-temperature oxide layer over the circuitry [Fig. 7 (center)]. Finally, contacts are opened for the sites and output pads. Sites are formed using iridium over titanium, and pads and are formed using gold over platinum and titanium. Finally, the field dielectrics are trimmed away and the silicon in the field area is recessed using a dry etch. The wafers at this point are thinned to about  $150 \mu\text{m}$  from the back and are then released in ethylenediamine pyrocatechol. This anisotropic etchant attacks the front and back of the wafer simultaneously, undercutting the probe shanks and other fine features



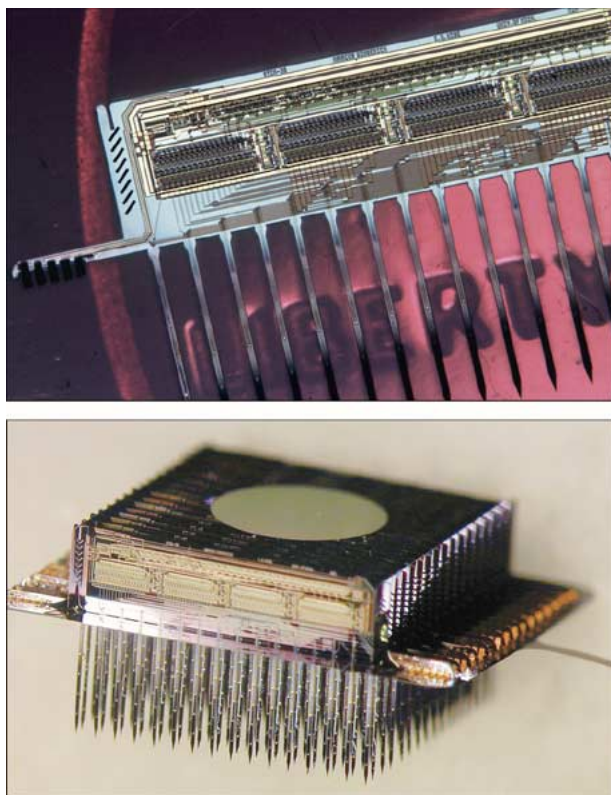


**Fig. 8.** Two views of a 3-D 1024-site 128-channel neuroelectronic interface.

from the front as it thins the wafer from the back. Finally, the probes separate from the wafer to leave the probe shanks at a thickness controlled by the etch-stop, while typically 40–50  $\mu\text{m}$  of silicon remains under the circuit areas. This process uses wafers of normal thickness with single-sided processing and high yield.

The insulation over the probe shanks is formed using an LPCVD oxide/nitride/oxide stress-compensated dielectric stack, whereas over the circuit area LTO is used with an electroplated gold shield, formed simultaneously with the output pads. In 3-D arrays, where several probes are microassembled into a platform that rides on the cortical surface, the back areas of the probes will eventually be sealed inside a glass cap. Hermetic sealing techniques are being developed for these structures as discussed below; in the meantime, they are potted in polymers such as silicone NuSil Med-4211 (Carpenteria, CA). For 3-D arrays [65], [66], wings on the probes are used to transfer leads on the probe to pads on an orthogonal platform using gold-plated tabs. Spacers are used to hold the probes parallel to each other. Fig. 8 shows a photograph of a 16-probe 128-shank 1024-site 3-D microassembled array. An alternative and important 3-D microstructure is the “Utah Electrode Array” [67], which is a batch-fabricated two-dimensional depth array formed using silicon posts created by sawing and etch-back. The individual posts are insulated with parylene and tipped with iridium. Each post electrode is isolated from neighboring electrodes using a mote of glass surrounding the electrode at its base. Arrays of 100 electrodes have been implanted for up to three years and have met with considerable success in both sensory and motor cortex [68].

### E. Drug Delivery and Microfluidics

For many applications, it is desirable to be able to control the chemical environment of the neurons in addition to interfacing with them electronically. It has been shown [69] that fluidic microchannels for drug delivery can be embedded in the Michigan probe substrates using only one masking step in addition to the eight normally used for a passive probe process. This mask opens a grid structure through a boron-doped surface layer at the start of the process, and a subsequent etching step (wet, dry, or a combination of the two) is used to undercut the grid and form a buried microchannel as shown in Fig. 9. Microflowmeters and outlet shutters can also be formed using two additional masks [70], [71], and test structures have been demonstrated for the formation of pumps and valves using the same process. Thus, the realization of probes containing electrical recording and stimulation along with complete duality in the chemical domain appears possible without prohibitive complexity in the overall process. The performance of these probes is being characterized *in vivo* in guinea pig inferior colliculus [72] as discussed below.

### III. MICROSYSTEM PACKAGING

Packaging implantable microsystems presents a number of special challenges [73], [74]. It must protect the implant for years or decades *in vivo*, be biocompatible, provide hermetically sealed feedthroughs for the required leads, and be very small. Wafer-level packaging techniques are, therefore, of great interest. Both organic and inorganic thin films and the use of protective shells around the sensitive components are being pursued. Some thin films are adequate for at least a few years, are easily deposited, and take very little volume. Protective shells sometimes make it difficult to transfer signals in and out of the package and may require an external antenna for wireless applications. Recently, wafer bonding and micromachining techniques have made it possible to realize miniature hermetic packages with the required feedthroughs. The capsules can be fabricated from a variety of materials, including metals, glass/ceramic, or silicon. A variety of material bonding techniques have been utilized for package formation [74], including silicon–glass bonding, glass frit bonding, and eutectic or solder bonding. Such capsules can provide a very reliable, long-term stable hermetic environment for the microsystem.

Electrostatic (anodic) bonding of glass (Pyrex 7740) to silicon is widely used [74]. Bonding is achieved when polished silicon and glass wafers are brought into intimate contact and a high voltage is applied across the sandwich to create a permanent chemical bond. Temperatures of 300–400  $^{\circ}\text{C}$  and voltages of 800–1500 V are typically used. The resulting electrostatic force pulls the silicon and glass together, creating a permanent chemical bond. This approach has been used to form sealed cavities for implantable microstimulators, with feedthroughs formed using polysilicon lines on a pitch of 5  $\mu\text{m}$  [75]. The lines are insulated with oxide/nitride/oxide as are the probes themselves. A layer of fine-grain



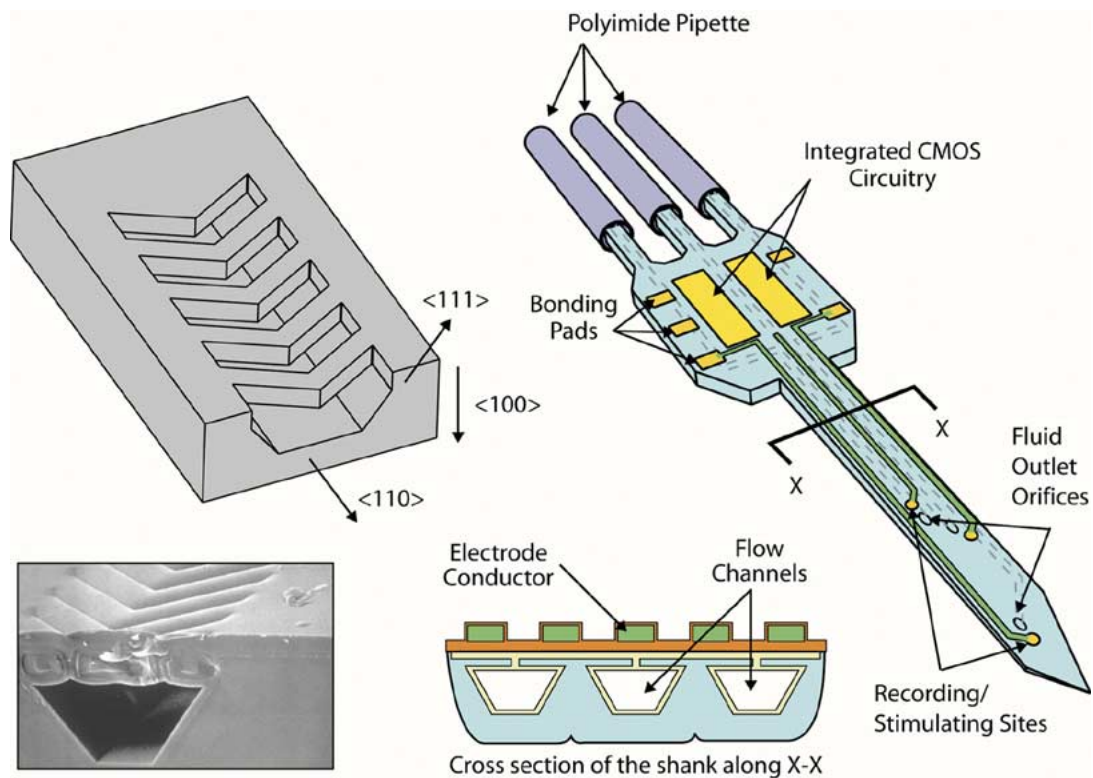


**Fig. 9.** Diagram of one structure used for realizing buried CVD-sealed microchannels for drug delivery in the silicon substrate along with a diagram of the resulting probe. Probes containing electrical recording/stimulating sites, orifice shutters, fluidic cables, and in-line flowmeters have now been realized.

polysilicon is deposited to act as the bonding surface. Accelerated tests in PBS have been performed at 85 °C and 95 °C and indicate that such packages can survive in salt water for many decades at body temperature [74], [76]. In addition, long-term testing of silicon–glass packages containing integrated wireless humidity sensors used for monitoring package hermeticity has been performed in guinea pigs. These tests have demonstrated that the packages remain hermetic for up to 22 mo (the maximum time guinea pigs could be kept alive) and do not elicit any profound adverse reaction from the body [74], [76].

The use of thin-film packaging for the probe circuitry is illustrated in Fig. 10 [74], [77]. Organic materials such as epoxies, silicones, polyimides, polyurethanes, and Parylene-C have been explored. They can be deposited at low temperatures, are conformal, and their characteristics can be modified for different applications; however, most of these films are not hermetic and are prone to moisture penetration. Inorganic materials such as silicon nitride, silicon carbide, polycrystalline diamond, metal thin films, and tantalum oxide are also very attractive and generally offer better long-term protection. Silicon and silicon carbide are resistant to corrosive environments but require very high temperatures to achieve reasonable deposition rates.

Silicon nitride has long been used for protection of ICs against moisture [74]. All tests to date indicate that silicon nitride is an excellent thin-film material for hermetic encapsulation even in very thin layers so long as the films are pin-hole free. Thin metal films [77] are also attractive because

they provide excellent barriers against moisture. The films can be deposited on polymers, but any polymer selected must exhibit good adhesion and must cure at a temperature higher than the remaining process steps to prevent subsequent bubbling of the polymer in process. Polyimide is attractive for its low dielectric constant and the fact that it can easily be spun cast into a thick film that cures above 350 °C. Gold can be used to encapsulate the polyimide and can easily be electroplated to form a high-density biocompatible film. This approach can create long-term packages at the wafer level and does not require bonding, high temperatures, or high voltages. Accelerated tests in salt water on active probes such as that shown in Fig. 10 [77] indicate that such packages can withstand exposure to salt water for at least 35 years. Pinholes are the most common form of failure, as indicated above.

#### IV. *IN VIVO* PROBE PERFORMANCE

The probes discussed in this paper are designed to interface with particular areas of the nervous system at the level of individual neurons or small populations of them. This joining of a nonbiological device to neural tissue is a decidedly nontrivial process that stands out among biomedical implants because the primary objective is to effect the reliable *transmission of information* between neurons and the external world. The fidelity of this transmission (the recording or stimulating performance of the probe) is intricately related to many factors, including probe location

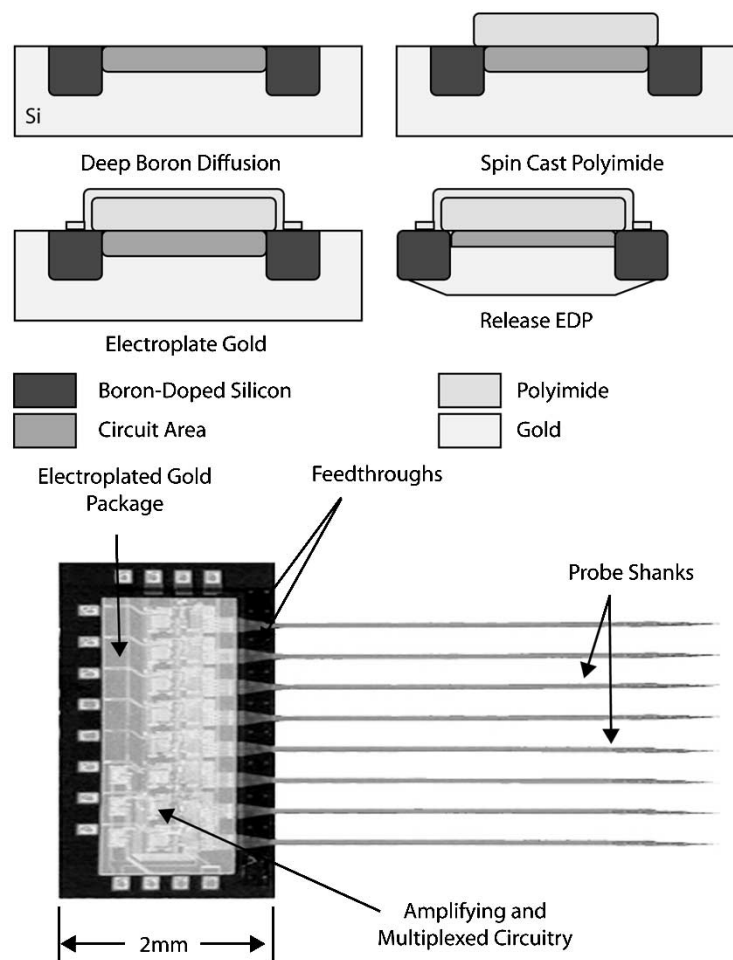


**Fig. 10.** Electroplated metal films used as hermetic packages for the protection of on-chip circuitry. (a) Cross-sectional view of the fabrication process for a gold-over-polymer package. (b) Fabricated probe with circuitry encapsulated using this process.

within the nervous system, site positioning with respect to the targeted neurons, injury responses elicited by the indwelling probe, surgical techniques for inserting and securing the device, and the supporting instrumentation and packaging [78], [79].

While the composition of the brain varies with location (and species), the human cerebral cortex may be used as a prototypical example of the microenvironment around an inserted probe. To a first approximation, there are approximately 30 000 neurons and  $2.4 \times 10^8$  synapses (assuming 8000 synapses/neuron) [80] in a cubic millimeter of the human cortex. Pyramidal neurons are the largest cells in the cortex, with bodies approximately  $10\text{--}30\text{ }\mu\text{m}$  in diameter. These cells compose the primary “output” neurons in the cortex and are the likely recording targets for neuroprosthetic microsystems. A Michigan probe shank with a cross section measuring  $15 \times 60\text{ }\mu\text{m}$  inserted 2 mm into cortex displaces  $0.0018\text{ mm}^3$  of cortical tissue (Fig. 11) and can, therefore, be expected to displace (or destroy) approximately 50 neurons and 400 000 synapses. Such a shank could typically contain eight or more sites, arranged in depth. Three of these penetrating shanks on  $150\text{-}\mu\text{m}$  centers displace  $0.0054\text{ mm}^3$ , or about 1.5% of a rectangular volume extending  $150\text{ }\mu\text{m}$  around the array cross-sectional

footprint and 2 mm deep. This volume is a somewhat arbitrary estimate of the “zone of influence” of the probe that includes the neurons that can be recorded by it [81], [82] as well as the region where a local tissue reaction might be elicited by its presence [83]. Cylindrical  $50\text{-}\mu\text{m}$ -diameter penetrating shanks (e.g., microwires), with only a single site, displace about twice the tissue of the silicon shank. Furthermore, even conservative lithography rules ( $1\text{-}\mu\text{m}$  features) can decrease the interconnect width on the shank by a factor of three, reducing the volume displacement of the silicon shank to about 0.5% and making it smaller than the microwire by a factor of nearly fifty on a per-site basis.

Beyond the relatively modest tissue displacement associated with a penetrating probe shank, inserting the probe into the brain invariably causes a stab wound that elicits an injury response and causes the formation of scar tissue around the device to wall it off from the surrounding brain. The stab wound involves incising the membranes that enclose the brain (the meninges: dura mater, subarachnoid mater, and pia mater), cellular damage, and microhemorrhages associated with piercing the microvasculature of the brain tissue. The injury response involves a complex and dynamic chemical signaling cascade that is an area of active research (e.g., [84]–[86]) beyond the scope of this

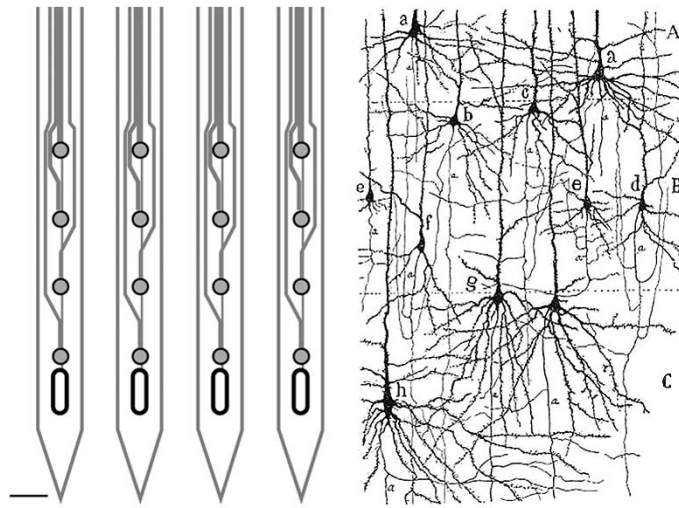


**Fig. 11.** A typical probe layout is shown with a thin section of the cerebral cortex to illustrate the basic spatial arrangement and scale of probe recording sites (dark circles) to cortical neurons (dark stained cells). The actual density of neurons and supporting cells is much greater than the density of stained cells in this cortical cross section.

paper. The effects of a pronounced response are least serious for stimulating sites (where the stimulating current can blow through the enveloping tissue layer) and most serious for small ( $< 100 \mu\text{m}^2$ ) single-unit recording sites, where the scar tissue can lead to a loss of recording ability. The tissue envelope is formed from epithelial cells and from glia, with a total thickness of a few micrometers. Since the injury response can be mitigated—but not completely eliminated—the engineering challenge is really to develop devices and techniques to *control* the tissue response to the degree required. Iridium recording sites are being coated with conductive polymers to improve recording stability and quality as part of ongoing efforts to develop techniques to facilitate mechanical stabilization of the probes in the brain and improve biological responses [87]. Silicon probes are attractive because their features can be engineered to optimize performance for a given application. Although the remainder of this section is restricted to a discussion of the *in vivo* performance of Michigan probes, a number of other probe structures have been developed elsewhere and presented in the literature. Of these, the Utah microelectrode array developed by Dr. R. Normann and colleagues is the most notable and well developed [67], [68], [88]–[93].

Over 6000 Michigan probes have been distributed by the Center for Neural Communication Technology<sup>1</sup> to over 180 investigators worldwide, where the probes are being used in a wide range of studies in animals. While the large majority of probes distributed to date have been passive, active probes and drug delivery probes are now being distributed as well. This distribution has resulted in over 200 journal papers and conference presentations in the neuroscience literature to date. Although over 150 different probe designs have been fabricated, a typical probe for acute animal use is a passive (no on-chip circuitry) 16-site device mounted on a miniature printed circuit board that connects to recording instrumentation and a manipulator. The effectiveness of

these probes for recording neuronal (unit) spike activity and local field potentials in diverse experimental preparations has been shown by many users. The size, shape, quality, and composition of the planar thin-film silicon device are clearly sufficient to permit positioning sites close to active neurons and transducing their electrical activity. While recording selectivity varies inversely with site size, the site position on the silicon substrate (tip, edge, middle) does not significantly affect recording quality. Many papers on the *in vivo* recording characteristics of the Michigan probes and experimental studies using them (e.g., [50], [94]–[100]) are found in the literature. The probes are in high demand, in part, because they can be designed with multiple precisely positioned sites to enable measurements not otherwise possible.

A growing number of neuroscientists are also using Michigan probes in semichronic animal experiments where it is important to record and/or stimulate in the same animal for periods of days to weeks. This application area requires the probes to be implanted and, in some cases, removed and reimplanted. Here, surgical techniques, injury responses, and packaging become more challenging. Dr. G. Buzsaki in the Center for Molecular and Behavioral Neuroscience, Rutgers University, Newark, NJ, is using both passive and active 64- and 96-site probes to chronically map neural activity (both slow-waves and single units) in the hippocampus of freely moving rats [94], [95] over periods of several weeks to explore short- and long-term memory formation.

The development of probes that can be permanently implanted to provide long-term neural interfaces is important and presents additional challenges beyond semichronic applications because packaging, surgical techniques, and dynamic injury responses all come to the forefront as additional factors in probe performance. At this point, the typical chronic probe configuration consists of a passive silicon penetrating microelectrode, an integrated thin silicon ribbon cable, and a commercial percutaneous connector. This system has been validated for recording neuronal action

<sup>1</sup><http://www.engin.umich.edu/facility/cnct/>

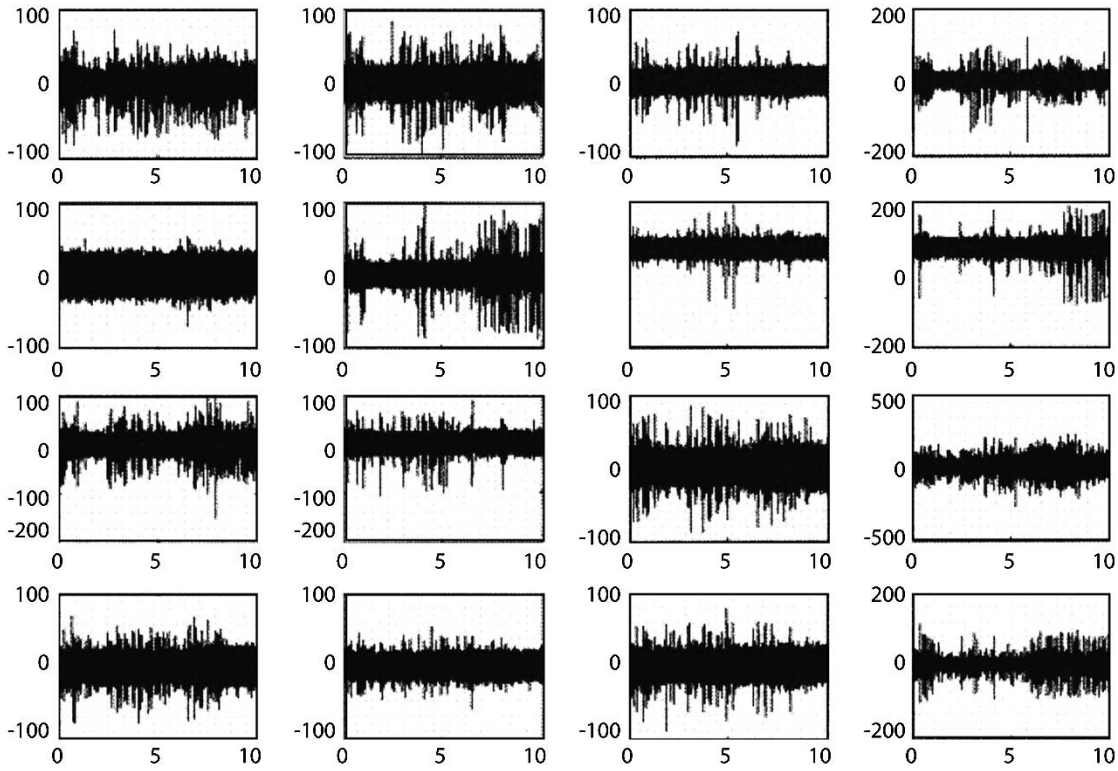


**Fig. 12.** Chronic extracellular recording with a passive silicon electrode array in rat cortex: 16 channels, 383 days post implant. Vertical: voltage ( $\mu\text{V}$ ); Horizontal: time (s).

potentials (unit spike recording) in the rat cerebral cortex for periods of more than one year [101]. One study used probes having four identical shanks spaced on  $150\text{-}\mu\text{m}$  centers, each with four regularly spaced recording sites separated by  $100\text{ }\mu\text{m}$  in depth. In a consecutive series of six rats, five of six of the implanted probes recorded neuronal spike activity for more than six weeks, with four of the implants (66%) remaining functional for more than 28 weeks. In each animal, more than 80% of the electrode sites recorded spike activity over sequential recording sessions during the postoperative period. One probe remained functional for over one year (383 days, Fig. 12); in each case the experiments ended for reasons other than probe failure. The quality of the day-to-day unit recordings was qualitatively comparable to other types of implantable microelectrodes, such as microwire arrays [6], but with multiple sites and far less insertion damage. Spike amplitudes ranged from  $50\text{--}800\text{ }\mu\text{V}$  peak-to-peak. Noise floors were nominally  $30\text{ }\mu\text{V}$  peak-to-peak and resulted from a combination of intrinsic site and instrumentation noise, as well as background neural activity. The signal-to-noise ratios (SNRs) were fairly stable over the duration of each implant with an initial mean SNR of 8.55 that gradually declined to 6.35 over the 54-week period. During this period, electrode site impedance magnitudes at  $1\text{ kHz}$  were generally found to increase during the first two weeks from initial values of  $1\text{ M}\Omega$ , stabilizing at  $1.6\text{--}2.0\text{ M}\Omega$ . A follow-up study, also in rats, characterized the recording performance of these probes in more detail over a 3-mo period and documented consistent high signal quality and reliability. This study also reported nominal tissue responses around the probe shanks

that are largely consistent to those reported with other types of penetrating probes [93], [103]. These results demonstrate that the silicon probes are sufficient for maintaining viable neural recording interfaces in the brain for periods that extend significantly beyond the initial acute injury response phase. This is an important finding because it provides a baseline for further development.

A variety of active probes have been fabricated to date and tested *in vitro* and *in vivo*. Fig. 13 [64] shows neural activity recorded with a multiplexed buffered probe in guinea pig cochlear nucleus, driven by white noise bursts. Channels 3 and 4 show neural activity with a high SNR; no neural activity is recorded on the first two channels because the corresponding sites were not in tissue due to the convexity of the cortical surface. These channels (which were nonetheless in fluid) are helpful in showing the noise of the system without background neural activity. For a bandwidth from  $300\text{ Hz}$  to  $3\text{ kHz}$ , the noise level of the external demultiplexing system is about  $3\text{ }\mu\text{V}_{\text{rms}}$ , while for a buffered output channel only (with no clock running) the measured noise is  $7\text{ }\mu\text{V}_{\text{rms}}$ . With the clock running but the on-chip multiplexer disabled, the overall noise level of the multiplexed system is still less than  $9\text{ }\mu\text{V}_{\text{rms}}$ . Hence, coupling from the external  $5\text{-V}$   $200\text{-kHz}$  clock into the recording channels after low-pass filtering is suppressed to a few parts per million as a result of the on-chip impedance transformation and the ground planes provided by the substrate and the surrounding fluid.

Michigan probes are also being used to deliver chemicals at the cellular level while electrically recording from and stimulating neurons *in vivo*. This work makes use of silicon probes that include integrated microchannels for



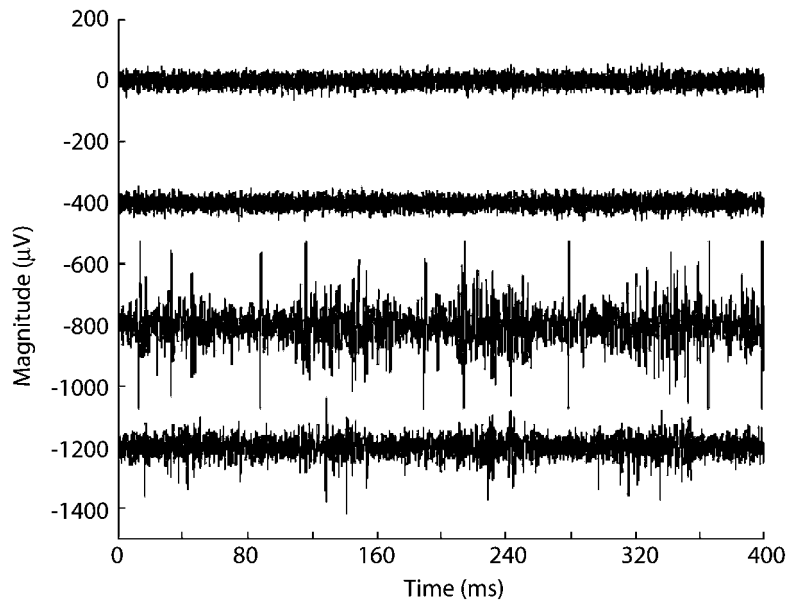


**Fig. 13.** Recordings from guinea pig cochlear nucleus using a multisite multishank multiplexed buffered probe. The tip two shanks were not in neural tissue and show the noise of the recording system without background neural noise. Multiplexing clock noise coupled into the recording channels is suppressed to the point that it does not significantly degrade the recorded signals.

fluid delivery [69], as noted above. A recent study tested the efficacy of the drug delivery system *in vivo* on neural discharge in the inferior colliculus of the guinea pig [72]. In nine of the ten applications of AMPA (an excitatory neurotransmitter agonist), there was a clear excitatory effect that was rapidly seen at all recording sites using the volumes tested, which were large relative to the volumes of cells. Fig. 14 shows the effects of a 2-nL application of 5  $\mu$ M of AMPA on neural discharge rates at five electrode sites recorded simultaneously. The application of AMPA produced excitation that grew during the first 10-s epoch at each of the five sites and then decayed, lasting for 20 s overall. Fig. 14 also shows results obtained with an equivalent control application of neutral Ringer solution alone (5 nL in 10 s). Larger doses (5 nL or more) of AMPA produced broader periods of excitation but the corresponding doses of Ringer solution showed some suppression of the discharge rate, probably as the dose pushed cells away from the region of the orifice. The site furthest from the orifice (Site 5) showed the least suppression. Without the integration of electrical recording with drug delivery, these volume effects could not have been observed.

## V. ON-CHIP CIRCUITRY

Since neural signals are typically from tens to hundreds of microvolts in amplitude, the first role for on-chip circuitry is to amplify the recorded signals and lower their impedance levels to make them less vulnerable to externally introduced noise. A second role is to multiplex the signals so many sites can be monitored from only a few external leads. Fig. 15 shows a block diagram of the circuitry on a 64-site 8-channel recording probe. The sites connect through a site-selection matrix to eight recording amplifiers, allowing the sites closest to neurons of interest to be selected. This site selector is controlled by an external clock and input data stream

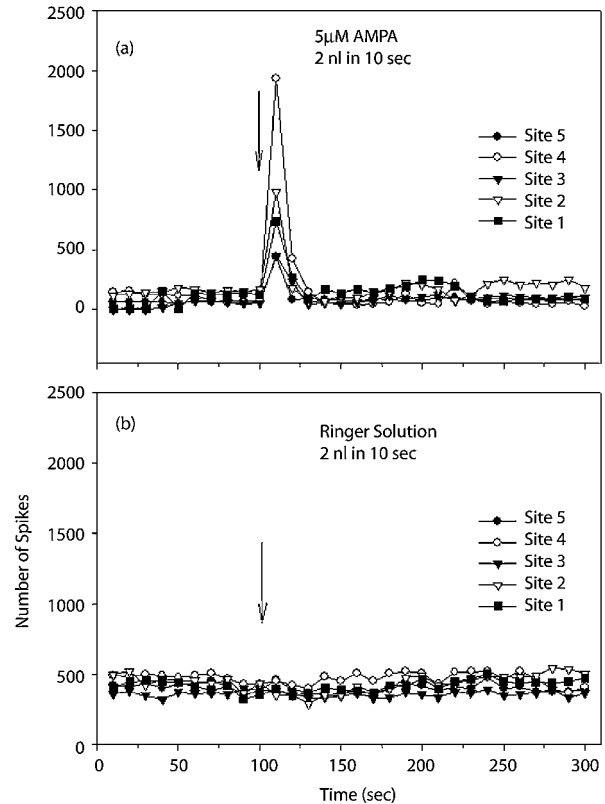


**Fig. 14.** Neural discharges from five recording sites in the inferior colliculus of a guinea pig before and after injection of: (a) 5  $\mu$ M of AMPA (excitatory neurotransmitter agonist, 2 nL in 10 s) and (b) Ringer solution alone (control, 2 nL in 10 s). Each data point represents 10 s of neural activity. The arrow denotes the time of ejection.

through a serial shift register and latch. The recording amplifiers boost the recorded signals by 40 dB while reducing their impedance amplitudes from a few megohms to a few hundred ohms. Next, the signals are time-multiplexed onto

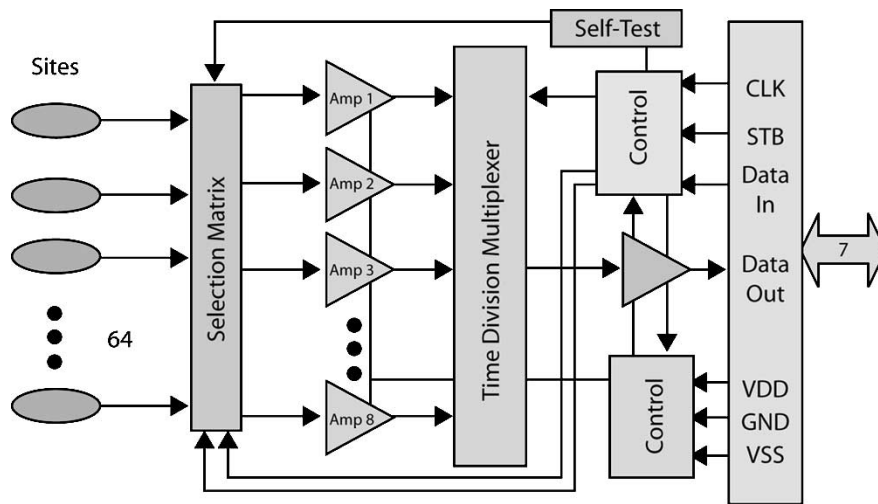


**Fig. 15.** Typical active recording probe, containing the functions of site selection, amplification, multiplexing, and self-test.

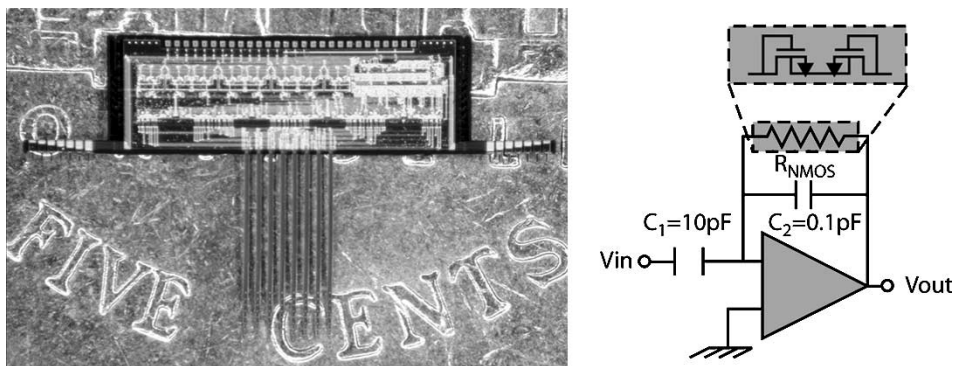


**Fig. 16.** A 64-site 8-channel recording probe, shown on a U.S. nickel. The probe dissipates 0.8 mW while providing a gain of 40 dB, over a bandwidth from 10 Hz to 10 kHz with an input noise less than  $10 \mu\text{V}_{\text{rms}}$ . A schematic of the recording amplifier is shown at the right.

a single output line where an output buffer boosts them by an additional 20 dB. Several command modes are typically present in such systems, including self-test, where a 1-kHz signal is coupled to the sites to allow external monitoring of their impedance levels, and stimulation, where current is driven through the sites in order to activate or clean them before or during use. This configuration requires seven output leads (VDD, VSS, GND, CLK, DataIn, DataOut, and Strobe) to monitor 64 sites. Using discrete leads, even this number of interconnects might be prohibitive; however, using micromachined cables or platform mounting it presents few problems.

The amplifier must provide stable gain and limit the high-frequency response to around 12 kHz to prevent aliasing in the multiplexer. It must also ac couple the signal to minimize offsets and suppress the unstable dc potential of the site. It must provide these features while not degrading overall system noise, occupying very little area, and dissipating less than 10 mW to avoid appreciable heating of the tissue. Temperature rises of more than  $2^\circ\text{C}$  would damage surrounding neurons. The capacitively coupled recording amplifier shown in Fig. 16 [104] provides these features. A 10-pF input capacitor and a 100-fF feedback capacitor set the midband gain at 40 dB. A diode-connected

subthreshold nMOS transistor in the feedback loop sets the lower band-pass corner at less than 10 Hz, while a Miller capacitor in the op-amp sets the high-frequency limit. A dc baseline rejection of more than  $\pm 500 \text{ mV}$  is achieved along with an input noise less than  $10 \mu\text{V}_{\text{rms}}$  [104]. The amplifier dissipates less than  $100 \mu\text{W}$  from  $\pm 1.5 \text{ V}$  supplies with a layout area in 1M/2P 3- $\mu\text{m}$  CMOS of  $0.08 \text{ mm}^2$ . Although the low-frequency cutoff in such amplifiers is not precise, it is reproducible enough, and since it is set using a transistor, it can be adjusted electronically depending on the nature of the signals to be recorded (field potentials or single units) [105]. Fig. 16 also shows a typical 64-site recording probe. The probe dissipates 0.8 mW and has a circuit area of  $4.3 \text{ mm}^2$  in 3- $\mu\text{m}$  technology.

Figs. 17 and 18 show the block diagram and photograph of a 64-site 8-channel stimulating probe. Here, most of the circuitry is digital. A serial input data stream is latched to provide command information. Using a 4-MHz clock, this can occur every  $4.5 \mu\text{sec}$ . Each command specifies a new current state for the probe and includes current amplitude and site address information [106]. Current can typically be set from  $-127 \mu\text{A}$  to  $+127 \mu\text{A}$  with  $\pm 1 \mu\text{A}$  resolution. In addition to launching a new stimulation pulse, commands can set different operating modes. Recording can be done from any site,

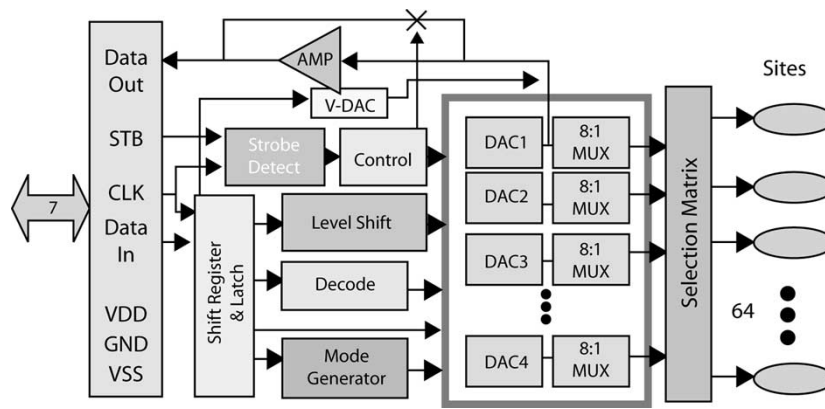


**Fig. 17.** A 64-site 8-channel stimulating probe. Operating from seven leads, a serial input data stream controls the current amplitudes launched from the various sites. Extensive self-test circuitry is included along with a variety of operating modes.

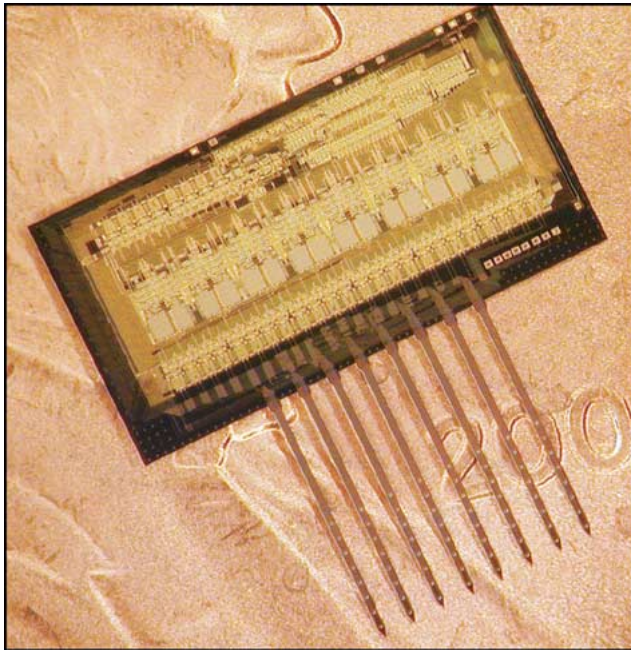


**Fig. 18.** A 64-site, 8-channel stimulating probe on a U.S. penny. The probe contains extensive self-test capabilities as well as the ability to record from any desired site.

or anodic bias can be applied to the sites over a range spanning the water window. A family of extended-range commands is also available to allow complete testability of the on-chip circuitry. Again, seven leads are required.

In the past, active probes have been primarily designed for recording or stimulation, with some stimulation or recording capability included on probes of the opposite type. However, in the future such devices will likely include full recording and full stimulating capability. Fabricating probes using 3- $\mu$ m features and single metal results in rather large circuit areas, which can compromise chronic implant performance since any rise above the cortical surface of more than 1 mm can make it difficult to keep the implant independent of the skull as the brain moves inside the cranial cavity. However, using the smaller feature sizes now current in industrial processes would reduce the circuit area dramatically and would allow room for more advanced on-chip signal processing.

Spike recognition circuitry is currently being designed for use on the platform to allow *in vivo* signal processing and interpretation and to ease telemetry requirements between the implant and the outside world.

## VI. WIRELESS INTERFACES

Wireless operation of implantable systems is key to their successful deployment in clinical applications. Wires, typically used for power and data transfer between the implant and the outside world, are a primary source of infection, failure, manufacturing cost, and discomfort to the patient. Wireless transmission of power and data circumvents all of these problems. Power and data signals can be transmitted using electromagnetic radio frequency (RF), infrared, or acoustic energy; however, wireless telemetry based on RF transmission between two closely coupled coils is most commonly used. A typical wireless interface must satisfy several basic requirements. First, sufficient power has to be transmitted to the implant to enable operation of its circuitry and, in the case of stimulation, deliver charge to the tissue. Second, the telemetry technique used must have sufficient range. This requirement depends on the application, but a range of a few centimeters is adequate for most prosthetic applications. Third, the wireless link should provide a high data transfer rate (bandwidth). This requirement is also application dependent, although in most emerging recording and stimulating systems, bandwidths in excess of 1–2 Mb/s are needed [107]–[109]. Fourth, the telemetry approach chosen should be immune to most environmental conditions and should be able to pass through tissue. Finally, the wireless link should be adaptable so it can satisfy the needs of different applications.

Several detailed studies of coupled coils for medical implant applications were carried out from the 1960s through the 1980s [110]–[113]. Most of these utilized antenna coils that were several centimeters in diameter, although more recent studies by Heetderks [114], Shah [115], and Neagu [116] explored much smaller coils for both power and data transmission for implantable neural prosthesis applications. Hochmair and Zierhofer discussed transcutaneous power and data transmission in a series of publications from 1984

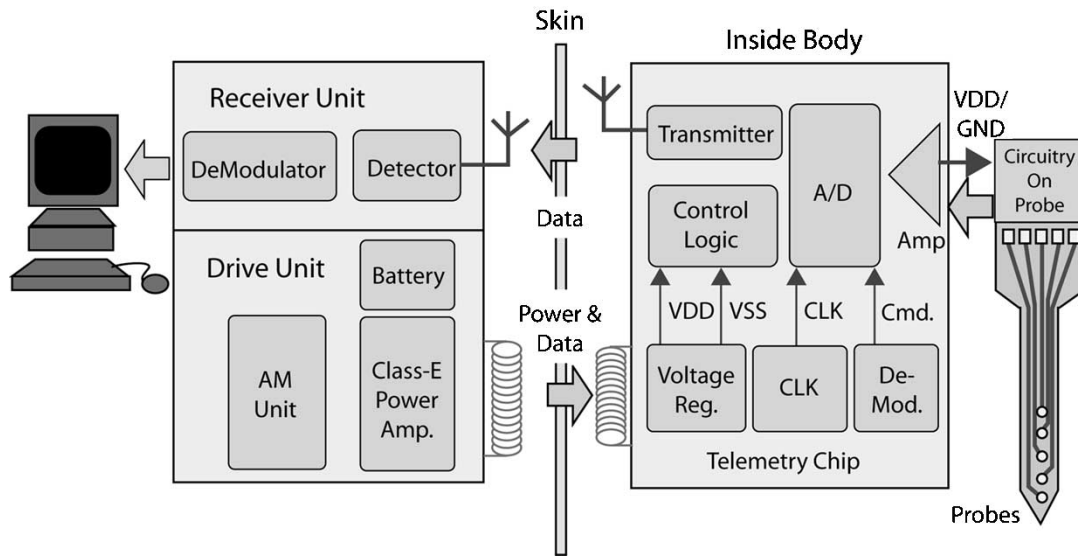


**Fig. 19.** Block diagram of an inductive RF telemetry link for an implantable microsystem.

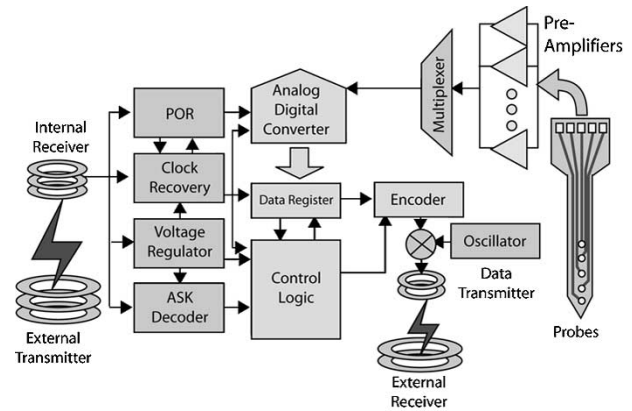
to 1996 [117]–[120]. Some researchers also developed complete implantable systems for specific applications ranging from cochlear implants to functional neural stimulators [115], [121]–[123].

Fig. 19 shows the diagram of a wireless telemetry link. Power and program data are transmitted via an inductive link to an implanted antenna (receiver). The implanted circuitry generates a dc power supply from the RF carrier, demodulates program data from the carrier, and generates a clock signal with which to operate the electronics. Data from the probe is digitized and transmitted back to the outside world over a second data link, often at a higher frequency. The external circuitry receives the transmitted data from the implant and reconstructs the transmitted signals.

#### A. Wireless Telemetry for Multichannel Neural Recording

A generalized system block diagram for an implantable multichannel neural recording system is shown in Fig. 20 [107]. The system may have multiple probes, each supporting several recording sites. The probes can be assembled into a silicon platform as discussed above, but they all interface to a single telemetry system. Buffered neural data from the probes are received by the platform circuitry, where the signals are converted into a digital format using on-chip analog-to-digital (A–D) converters [124]. It is also possible to transmit the recorded signals in analog form [125]; however, for large numbers of channels and when digitization is necessary for *in vivo* signal processing, an on-chip A–D converter is desirable.

One of the most important circuit blocks of a wireless neural recording system is the voltage regulator. The regulator should produce a stable, low-noise voltage level (better than 8 b of resolution) without the need for external hybrid components and with low power consumption. Since the power received by the implant is limited and the induced voltage across the receiver coil is relatively low, a low drop-out series regulator has been developed as shown in Fig. 21 [107]. The implanted receiver coil, diode D1



**Fig. 20.** Circuit diagram for a wireless multichannel neural recording system.

and capacitor C1, form a half-wave rectifier. The op-amp operates in a negative feedback loop to adjust the current through the pass transistor  $M_{\text{pass}}$  so that the regulated voltage  $V_{\text{dd}}$  can be kept constant. A voltage doubler block, made up of C2 and MD, is used to provide a higher supply voltage to the op-amp, which consumes very little power, to accommodate the voltage drop across the switch. A bandgap reference circuit is used to generate a reference voltage, and a regulated voltage supply is produced by the op-amp and the bandgap reference circuit as shown. This configuration can lead to a more accurate and stable voltage reference. A startup circuit is necessary to drive the circuit out of the zero quiescent state. The regulator provides a line regulation of 3 mV/V, load regulation of 8 mV/mA, and ripple rejection of 45 dB.

The details of the data demodulator, clock circuitry, and A–D circuitry are provided in [109]. An amplitude-shift-keyed (ASK) demodulator decodes data from the modulated RF carrier. For an RF carrier frequency of 4 MHz, a data rate of 60 kb/s has been achieved using this simple demodulator. The clock needed for the operation of the circuitry is derived from the RF carrier. Neural data is



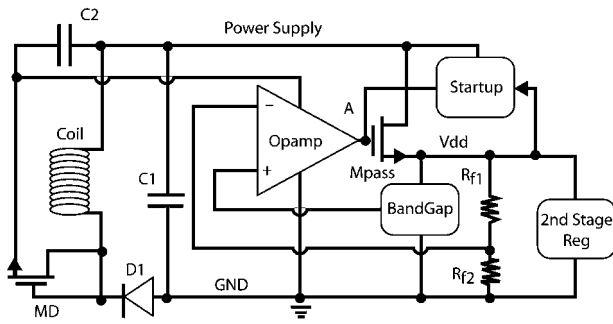


Fig. 21. Circuit diagram of a low drop-out voltage regulator.

digitized using a 10b charge-redistribution A–D converter (ADC). The ADC operates at a 4-MHz clock and consumes 1.41 mW from a 3-V power supply. It has a conversion speed of 250 ksamples/s and an accuracy of better than 9b, which is sufficient for neural recording applications.

There are primarily two methods for retrieving data from an implant: passive impedance reflection and active transmission. Passive transmission is also referred to as “load shift keying” [126], where changes in the loading of the implanted secondary coil are reflected back as a change in the impedance of the primary coil (outside the body). External decoding circuitry can sense the loading changes to detect the transmitted data. In active transmission, the implant circuitry drives an internal antenna to actively transmit the signals to the external receiver, where the carrier is modulated in amplitude, frequency, or phase. Active transmission consumes more power but achieves higher data rates and greater range than passive transmission [107].

These circuit blocks can be used in a variety of implantable systems to provide regulated supply voltages, data, and clock to the implant, and to digitize sensor data and transmit results to the outside world. The interface circuits have been integrated in a 0.8- $\mu\text{m}$  CMOS process on a chip measuring  $2.2 \times 2.2$  mm [107]. The chip can be mounted on the platform shown in Fig. 1. An external class-E power amplifier is used to drive an external transmitter coil to deliver power to the implant. On-chip regulators operate well even when the induced voltage across the receiver coil ranges from 6 to 15 V. The measured power consumptions for the front-end and on-chip transmitter are 476  $\mu\text{W}$  and 1.693 mW, respectively; the power dissipation of the 10b ADC is 1.4 mW at a clock frequency of 4 MHz. Fig. 22 shows the chip photograph.

### B. Wireless Telemetry for Multichannel Neural Stimulation

Wireless operation of multichannel stimulating arrays is critical in many prosthetic applications. The challenges here are similar to those in recording systems. Power and data are derived from a modulated RF carrier and used to operate the implanted electronics and deliver charge through the stimulating sites to the tissue. The required bandwidth can be quite large in systems having large numbers of sites. The block diagram of a generic chip for use with a multichannel multishank microprobe such as that in Fig. 18 is shown in

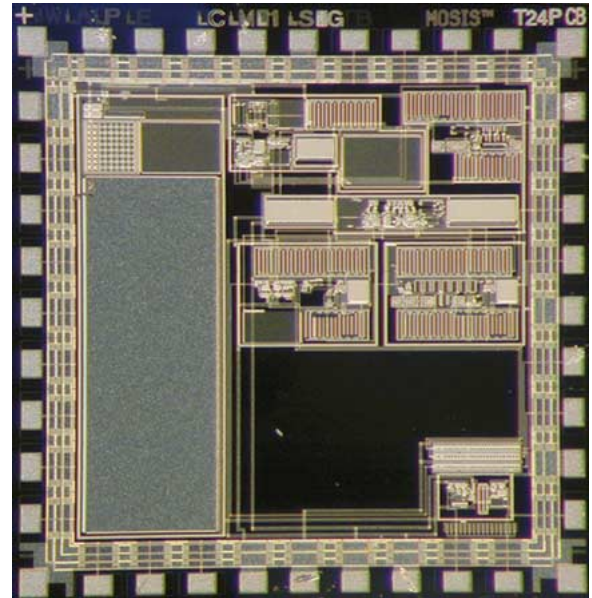


Fig. 22. IC chip implementing the functions needed for a wireless neural recording system.

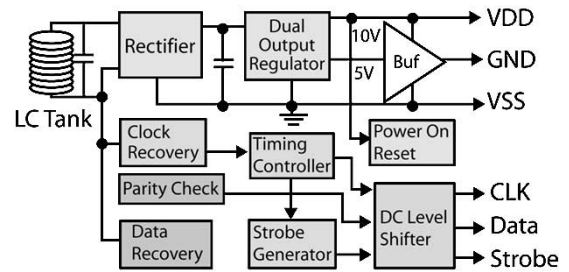
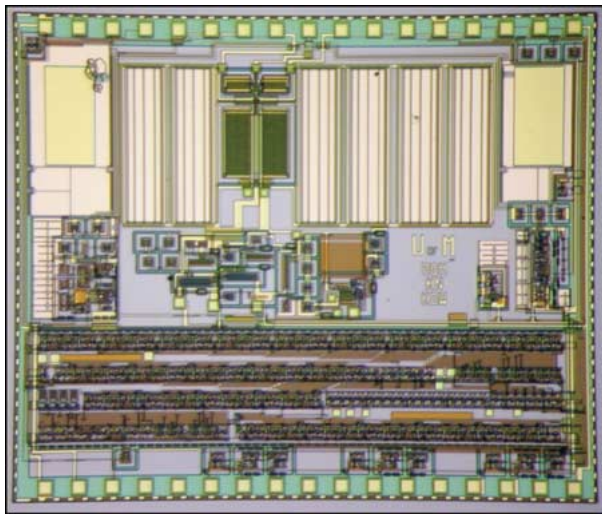


Fig. 23. Generic wireless interface for multichannel stimulating probes.

Fig. 23 [127]. Power and program data are received through a solenoid coil on the platform. The carrier is rectified and a regulator generates  $\pm 5$  V supplies for the probe. Data and clock signals are derived from the carrier and a strobe is generated for the probe. Parity checks are performed to ensure the validity of the incoming data. Fig. 24 shows the wireless interface, implemented on a  $3 \times 3.5$  mm chip fabricated in 3- $\mu\text{m}$  CMOS. Up to 5 mA can be generated by each of the supplies. The wireless interface would normally be placed on the platform shown in Fig. 1 as a hybrid chip; however, for other situations, versions have also been designed and implemented on the probe itself [108].

One of the main challenges in multichannel stimulating systems is the need for bandwidths of at least 1–2 Mb/s, which can be readily accomplished by increasing the carrier frequency. However, for ranges of a few centimeters, the high attenuation of RF signals in biological tissue dictates carrier frequencies below 10 MHz. To overcome this limitation, a new approach for data transfer based on frequency shift keying (FSK), instead of ASK, has been developed [109]. In this approach, the carrier is shifted between two frequencies that are different by a factor of two. The data transmission rate is set by how fast the frequency can be switched. This



**Fig. 24.** A 3- × 3.5-mm chip in 3- $\mu$ m CMOS implementing the interface for a wireless stimulating probe.

switching can be performed at frequencies of up to 60% of the carrier, implying that bandwidths as high as 2–3 MHz can be achieved for carrier frequencies below 5 MHz.

## VII. CONCLUSION

This paper has described the development of chronically implantable microsystems for electronically interfacing to the central nervous system. Single-unit recording in behaving animals for more than a year is now possible, and continuing improvements in bioactive coatings and implantation techniques should extend this much further. Active probes containing circuitry for site selection, amplification, stimulus generation, and multiplexing can now be fabricated with high yield and are beginning to be applied, making possible studies using dozens to hundreds of sites. Three-dimensional microassembly techniques have been defined that permit the realization of electrode arrays dense enough to monitor (or stimulate) virtually every cell within a block of tissue while displacing less than one percent of the tissue volume. Packaging techniques for full microsystems containing embedded signal processing, spike recognition, and wireless transmission of power and bidirectional data are consistent with mean times to failure *in vivo* of many decades. Telemetry interfaces for both stimulation and recording have been defined at the prototype level, and the realization of button-size wireless implants is a near-term prospect. These bioMEMS devices are already yielding important advances in our understanding of neural systems and can be expected to lead to real breakthroughs in the future as the number of sites is increased, shank sizes are scaled down to decrease tissue trauma, and *in vivo* signal processing and telemetry are used for longer-term experiments in unrestrained behaving animals.

While much has been accomplished, many challenges remain, especially for neural prosthesis applications. Improved probe designs, implantation techniques, and chip coatings are needed to minimize tissue reactions (injury responses) over long implant periods and improve the physical probe–tissue

interface. This is perhaps the most serious challenge facing these devices for prosthetic use. Dielectric coatings and other packaging techniques for the probes must be validated over decades. Increased transmission bandwidth in the telemetry interfaces will be a continuing need to permit increased data flow, and *in vivo* spike recognition and micropower signal processing circuitry must be developed. Finally, microfluidic systems for drug delivery and chemical sensing at the cellular level are still at a very early stage of development. The challenges associated with realizing such systems using processes that are simple enough to be practical are many, but important first steps have been taken. As work continues in all these areas and as full microsystems move from research prototypes to widely used tools in neuroscience, we can hope that they will also set the stage for prosthetic devices capable of treating some of humankind's most serious and intractable disorders. The coming decade may indeed see some very real miracles in this area of health care.

## ACKNOWLEDGMENT

The authors would like to thank Dr. F. T. Hambrecht and Dr. W. J. Heetderks of the Neural Prosthesis Program, NINDS, for their encouragement, patience, and support of this work over many years. The authors would also like to thank the many faculty, staff, and doctoral students who have contributed in so many important ways to the results reported here.

## REFERENCES

- [1] B. Franklin, "An account of the effects of electricity in paralytic cases," *Philos. Trans.*, vol. 50, pp. 481–483, 1759.
- [2] R. C. Gesteland, B. Howland, J. Y. Lettvin, and W. H. Pitts, "Comments on microelectrodes," *Proc. IRE*, vol. 47, pp. 1856–1862, 1959.
- [3] C. A. Terzuolo and T. Araki, "An analysis of intra-versus extra-cellular potential changes associated with activity of single spinal motoneurons," *Ann. NY Acad. Sci.*, vol. 94, pp. 547–558, 1963.
- [4] M. Verseano and K. Negishi, "Neuronal activity in cortical and thalamic networks," *J. Gen. Physiol.*, vol. 43, pp. 177–195, 1960.
- [5] M. A. Nicolelis, A. A. Ghazanfar, B. M. Faggin, S. Votaw, and L. M. Oliveira, "Reconstructing the engram: Simultaneous, multisite, many single neuron recordings," *Neuron*, vol. 18, pp. 529–537, Apr. 1997.
- [6] J. C. Williams, R. L. Rennaker, and D. R. Kipke, "Long-term neural recording characteristics of wire microelectrode arrays implanted in cerebral cortex," *Brain Res. Protocols*, vol. 4, pp. 303–313, Dec. 1999.
- [7] I. Porada, I. Bondar, W. B. Spatz, and J. Kruger, "Rabbit and monkey visual cortex: More than a year of recording with up to 64 microelectrodes," *J. Neurosci. Methods*, vol. 95, pp. 13–28, 1999.
- [8] M. P. Lepselter, "Beam-lead technology," *Bell Syst. Tech. J.*, vol. 45, pp. 233–254, Feb. 1966.
- [9] K. D. Wise, J. B. Angell, and A. Starr, "An integrated circuit approach to extracellular microelectrodes," in *8th Int. Conf. Engineering Medicine and Biology*, 1969, p. 14.5.
- [10] —, "An integrated circuit approach to extracellular microelectrodes," *IEEE Trans. Biomed. Eng.*, vol. BME-17, pp. 238–247, July 1970.
- [11] K. D. Wise and J. B. Angell, "A low-capacitance multielectrode probe for use in extracellular neurophysiology," *IEEE Trans. Biomed. Eng.*, vol. BME-22, pp. 212–219, May 1975.
- [12] W. F. House and K. I. Berliner, "Cochlear implants: From idea to clinical practice," in *Cochlear Implants: A Practical Guide*, H. Cooper, Ed. San Diego, CA: Singular, 1991, pp. 9–33.

- [13] F. B. Simmons, "Electrical stimulation of the auditory nerve in man," *Arch. Otolaryng.*, vol. 84, pp. 2–54, 1966.
- [14] F. B. Simmons, C. J. Mongeon, W. R. Lewis, and D. A. Huntington, "Electrical stimulation of acoustical nerve and inferior colliculus: Results in man," *Arch. Otolaryngol.*, vol. 79, pp. 559–567, 1964.
- [15] G. S. Brindley and W. S. Lewin, "The sensations produced by electrical stimulation of the visual cortex," *J. Physiol.*, vol. 196, pp. 479–493, May 1968.
- [16] F. A. Spelman, "The past, present, and future of cochlear prostheses," *IEEE Eng. Med. Biol. Mag.*, pp. 27–33, May 1999.
- [17] W. Lui, "Retinal implant: Bridging engineering and medicine," in *Proc. IEEE Int. Electron Devices Meeting*, 2002, pp. 492–495.
- [18] E. Margalit, M. Maia, J. D. Weiland, R. J. Greenberg, G. Y. Fujii, G. Torres, D. V. Piyathaisere, T. M. O'Hearn, W. Liu, G. Lazzi, G. Dagnelie, D. A. Scribner, E. de Juan Jr., and M. S. Humayun, "Retinal prosthesis for the blind," *Surv. Ophthalmol.*, vol. 47, no. 4, pp. 335–356, 2002.
- [19] P. Limousin, P. Krack, P. Pollack, A. Benazzouz, C. Ardouin, D. Hoffmann, and A. Benabid, "Electrical stimulation of the subthalamic nucleus in advanced Parkinson's disease," *New Eng. J. Med.*, vol. 339, pp. 1105–1111, 1998.
- [20] J. K. Chapin, K. A. Moxon, R. S. Markowitz, and M. A. Nicolelis, "Real-time control of a robot arm using simultaneously recorded neurons in the motor cortex," *Nature Neurosci.*, vol. 2, pp. 664–670, July 1999.
- [21] M. D. Serruya, N. G. Hatsopoulos, L. Paninski, M. R. Fellows, and J. P. Donoghue, "Instant neural control of a movement signal," *Nature*, vol. 416, pp. 141–142, Mar. 2002.
- [22] D. M. Taylor, S. I. Tillery, and A. B. Schwartz, "Direct cortical control of 3-D neuroprosthetic devices," *Science*, vol. 296, pp. 1829–1832, June 2002.
- [23] K. Frank and M. C. Becker, "Microelectrodes for recording and stimulation," in *Physical Techniques in Biological Research*, W. L. Nastuk, Ed. New York: Academic, 1964, vol. 5.
- [24] J. R. M. Delgado, "Electrodes for extracellular recording and stimulation," in *Physical Techniques in Biological Research*, W. L. Nastuk, Ed. New York: Academic, 1964, vol. 5.
- [25] D. A. Robinson, "The electrical properties of metal microelectrodes," *Proc. IEEE*, vol. 56, pp. 1065–1071, June 1968.
- [26] O. F. Schanne, M. Lavallee, R. Laprade, and S. Gagne, "Electrical properties of glass microelectrodes," *Proc. IEEE*, vol. 56, pp. 1072–1082, June 1968.
- [27] D. J. Edell, "A peripheral nerve information transducer for amputees: Long-term multichannel recordings from rabbit peripheral nerves," *IEEE Trans. Biomed. Eng.*, vol. BME-33, pp. 203–214, Feb. 1986.
- [28] G. A. May, S. A. Shamma, and R. L. White, "A tantalum-on-sapphire microelectrode array," *IEEE Trans. Electron Devices*, vol. ED-26, pp. 1932–1939, Dec. 1979.
- [29] O. J. Prohaska, F. Olcaytug, P. Pfundner, and H. Dragaun, "Thin-film multiple electrode probes: Possibilities and limitations," *IEEE Trans. Biomed. Eng.*, vol. BME-33, pp. 223–229, Feb. 1986.
- [30] M. Kuperstein and D. A. Whittington, "A practical 24-channel microelectrode for neural recording in-vivo," *IEEE Trans. Biomed. Eng.*, vol. BME-28, pp. 288–293, Mar. 1981.
- [31] N. A. Blum, B. G. Carkhuff, H. K. Charles, R. L. Edwards, and R. A. Meyer, "Multisite microprobes for neural recordings," *IEEE Trans. Biomed. Eng.*, vol. 38, pp. 68–74, Jan. 1991.
- [32] R. S. Pickard, P. L. Joseph, A. J. Collins, and R. C. J. Hicks, "Flexible printed-circuit probe for electrophysiology," *Med. Biol. Eng. Comput.*, vol. 17, pp. 261–267, 1979.
- [33] K. E. Petersen, "Silicon as a mechanical material," *Proc. IEEE*, vol. 70, pp. 420–457, May 1982.
- [34] D. J. Edell, private communication.
- [35] K. Najafi, J. Ji, and K. D. Wise, "Scaling limitations of silicon multichannel recording probes," *IEEE Trans. Biomed. Eng.*, vol. 37, pp. 1–11, Jan. 1990.
- [36] C. Huang and K. Najafi, "Fabrication of ultrathin  $p++$  silicon microstructures using ion implantation and boron etch-stop," *J. Microelectromech. Systems*, vol. 10, pp. 532–537, Dec. 2001.
- [37] K. Najafi and J. F. Hetke, "Strength characterization of silicon microprobes in neurophysiological tissues," *IEEE Trans. Biomed. Eng.*, vol. 37, pp. 474–481, May 1990.
- [38] D. T. Kewley, M. D. Hills, D. A. Borkholder, I. E. Opris, N. I. Maluf, C. W. Stormont, J. M. Bower, and G. T. A. Kovacs, "Plasma-etched neural probes," *Sens. Actuators A*, vol. 58, pp. 27–35, 1997.
- [39] T. H. Yoon, E. J. Hwang, D. Y. Shin, S. I. Park, S. J. Oh, S. C. Jung, H. C. Shin, and S. J. Kim, "A micromachined silicon depth probe for multichannel neural recording," *IEEE Trans. Biomed. Eng.*, vol. 47, pp. 1082–1087, Aug. 2000.
- [40] P. Norlin, M. Kindlundh, A. Mouroux, K. Yoshida, and U. G. Hofmann, "A 32-site neural recording probe fabricated by DRIE of SOI substrates," *J. Micromech. Microeng.*, vol. 12, pp. 414–419, 2002.
- [41] K. C. Cheung, K. Djupsund, Y. Dan, and L. P. Lee, "Implantable multichannel electrode array based on SOI technology," *J. Microelectromech. Systems*, vol. 12, pp. 179–184, Apr. 2003.
- [42] E. M. Maynard, E. Fernandez, and R. A. Normann, "A technique to prevent dural adhesions to chronically implanted microelectrode arrays," *J. Neurosci. Methods*, vol. 97, pp. 93–101, 2000.
- [43] E. M. Schmidt, J. S. McIntosh, and M. J. Bak, "Long-term implants of parylene-C coated microelectrodes," *Med. Biol. Eng.*, vol. 26, pp. 96–101, 1988.
- [44] J. F. Hetke, J. L. Lund, K. Najafi, K. D. Wise, and D. J. Anderson, "Silicon ribbon cables for chronically implantable microelectrode arrays," *IEEE Trans. Biomed. Eng.*, vol. 41, no. 4, pp. 314–321, Apr. 1994.
- [45] R. J. Vetter, J. C. Williams, J. F. Hetke, and D. R. Kipke, "Long-term recording properties of implantable thin-film silicon microelectrode arrays in auditory cortex," *Soc. Neurosci. Abstr.*, 2002.
- [46] P. J. Rousche, D. S. Pellinen, D. P. Pivin Jr., J. C. Williams, R. J. Vetter, and D. R. Kirke, "Flexible polyimide-based intracortical electrode arrays with bioactive capability," *IEEE Trans. Biomed. Eng.*, vol. 48, pp. 361–371, Mar. 2001.
- [47] T. Stieglitz, H. Beutel, and J.-U. Meyer, "A flexible, light-weight multichannel sieve electrode with integrated cables for interfacing regenerating peripheral nerves," *Sens. Actuators A*, vol. 60, pp. 240–243, 1997.
- [48] J. F. Hetke, J. C. Williams, D. S. Pellinen, R. J. Vetter, and D. R. Kipke, "3-D silicon probe array with hybrid polymer interconnect for chronic cortical recording," in *Proc. IEEE EMBS Special Topic Conf. Neural Engineering*, 2003, pp. 181–184.
- [49] M. Maghribi, J. Hamilton, D. Polla, K. Rose, T. Wilson, and P. Krulvitch, "Stretchable microelectrode array," in *Proc. Int. IEEE-EMBS Special Topics Conf. Microtechnologies Medicine and Biology*, 2002, pp. 80–83.
- [50] K. L. Drake, K. D. Wise, J. Farraye, D. J. Anderson, and S. L. Bement, "Performance of planar multisite microprobes in recording extracellular single-unit intracortical activity," *IEEE Trans. Biomed. Eng.*, vol. 35, pp. 719–732, Sept. 1988.
- [51] B. Ziaie, J. Von Arx, and K. Najafi, "A micro-fabricated planar high-current IrOx stimulating microelectrode," in *Proc. IEEE Engineering Medicine and Biology (EMBS) Conf.*, vol. 1, 1996, pp. 270–271.
- [52] S. J. Tanghe, "Micromachined silicon stimulating probes with CMOS circuitry for use in the central nervous system," Ph.D. dissertation, University of Michigan, Ann Arbor, 1992.
- [53] L. S. Robblee and T. L. Rose, "Electrochemical guidelines for selection of protocols and electrode materials for neural stimulation," in *Neural Prosthesis: Fundamental Studies*, W. Agnew and D. B. McCreery, Eds. Englewood Cliffs, NJ: Prentice-Hall, 1990, ch. 2.
- [54] J. D. Weiland and D. J. Anderson, "Chronic neural stimulation with thin-film, iridium oxide electrodes," *IEEE Trans. Biomed. Eng.*, vol. 47, pp. 911–918, 2000.
- [55] D. J. Anderson, K. Najafi, S. J. Tanghe, D. A. Evans, K. L. Levy, J. F. Hetke, X. L. Xue, J. J. Zappia, and K. D. Wise, "Batch-fabricated thin-film electrodes for stimulation of the central auditory system," *IEEE Trans. Biomed. Eng.*, vol. 36, pp. 693–704, July 1989.
- [56] L. M. Schiavone, W. C. Dautremont-Smith, G. Beni, and J. L. Shay, "Improved electrochromic behavior of reactively sputtered iridium oxide films," *J. Electrochem. Soc.*, vol. 128, no. 6, pp. 1339–1342, 1981.
- [57] B. Aurian-Blajeni, M. M. Boucher, A. G. Kimball, and L. S. Robblee, "Physiochemical characterization of sputtered iridium oxide," *J. Mater. Res.*, vol. 4, no. 2, pp. 440–446, 1989.
- [58] R. D. Meyer, S. F. Cogan, T. H. Nguyen, and R. D. Rauh, "Electrodeposited iridium oxide for neural stimulation and recording electrodes," *IEEE Trans. Neural Syst. Rehab. Eng.*, vol. 9, pp. 2–11, Mar. 2001.
- [59] P. G. Pickup and V. I. Birss, "A model for anodic hydrous oxide growth at iridium," *J. Electroanal. Chem.*, vol. 220, pp. 83–100, 1987.

- [60] —, "The influence of the aqueous growth medium on the growth rate, composition, and structure of hydrous iridium oxide films," *J. Electrochem. Soc.*, vol. 135, no. 1, pp. 126–133, 1988.
- [61] X. Beebe and T. L. Rose, "Charge injection limits of activated iridium oxide electrodes with 0.2 ms pulses in bicarbonate buffered saline," *IEEE Trans. Biomed. Eng.*, vol. 35, no. 6, pp. 494–495, June 1988.
- [62] L. S. Robblee, J. L. Lefko, and S. B. Brummer, "Activated Ir: An electrode suitable for reversible charge injection in saline solution," *J. Electrochem. Soc.*, vol. 130, no. 3, pp. 731–733, 1983.
- [63] C. Kim and K. D. Wise, "A 64-site multishank CMOS low-profile neural stimulating probe," *IEEE J. Solid-State Circuits*, vol. 31, pp. 1230–1238, Sept. 1996.
- [64] Q. Bai and K. D. Wise, "Single-unit recording with active microelectrode arrays," *IEEE Trans. Biomed. Eng.*, pp. 911–920, Aug. 2001.
- [65] —, "A high-yield microassembly structure for three-dimensional microelectrode arrays," *IEEE Trans. Biomed. Eng.*, pp. 281–289, Mar. 2000.
- [66] M. D. Gingerich, J. F. Hetke, D. J. Anderson, and K. D. Wise, "A 256-site 3D CMOS microelectrode array for multipoint stimulation and recording in the central nervous system," presented at the Int. Conf. Solid-State Sensors and Actuators, Munich, Germany, 2001.
- [67] K. E. Jones, P. K. Campbell, and R. A. Normann, "A glass/silicon composite intracortical electrode array," *Ann. Biomed. Eng.*, vol. 20, pp. 423–37, 1992.
- [68] R. A. Normann, "Microfabricated electrode arrays for restoring lost sensory and motor functions," in *Dig. IEEE Int. Conf. Solid-State Sensors, Actuators, and Microsystems*, 2003, pp. 959–962.
- [69] J. K. Chen, K. D. Wise, J. F. Hetke, and S. C. Bledsoe Jr., "A multichannel neural probe for selective chemical delivery at the cellular level," *IEEE Trans. Biomed. Eng.*, pp. 760–769, Aug. 1997.
- [70] D. Papageorgiou, S. C. Bledsoe, M. Gulari, J. F. Hetke, D. J. Anderson, and K. D. Wise, "A shuttered probe with in-line flowmeters for chronic in-vivo drug delivery," in *Proc. IEEE MEMS Conf.*, 2001, pp. 212–215.
- [71] D. Papageorgiou, S. Bledsoe, K. D. Wise, and D. J. Anderson, "A process-compatible passive shutter for buried-channel chemical delivery probes," in *Proc. Int. Conf. Engineering Medicine and Biology*, 1999, p. 835.
- [72] R. Rathnasingham, S. C. Bledsoe, J. D. McLaren, and D. R. Kipke, "Characterization of implantable microfabricated fluid delivery devices," in *IEEE Trans. Biomed. Eng.*, 2003. In press.
- [73] W. H. Ko and T. M. Spears, "Packaging materials and techniques for implantable instruments," *Eng. Med. Biol.*, vol. 2, pp. 24–38, Mar. 1983.
- [74] K. Najafi, "Micropackaging technologies for integrated microsystems: Applications to MEMS and MOEMS," presented at the SPIE Micromachining and Microfabrication Symp., San Jose, CA, 2003.
- [75] B. Ziaie, J. Von Arx, M. Dokmeci, and K. Najafi, "A hermetic glass-silicon micropackage with high-density on-chip feedthroughs for sensors and actuators," *J. Micromech. Systems*, vol. 5, pp. 166–179, 1996.
- [76] T. J. Harpster and K. Najafi, "Long-term testing of hermetic anodically bonded glass-silicon packages," in *Tech. Dig. IEEE 2002 Int. Conf. Micro Electro Mechanical Systems (MEMS 2002)*, pp. 423–426.
- [77] B. H. Stark and K. Najafi, "An ultra-thin hermetic package utilizing electroplated gold," in *Dig. 11th IEEE Int. Conf. Solid-State Sensors and Actuators (Transducers '01)*, 2001, pp. 194–197.
- [78] D. J. Edell, V. V. Toi, V. M. McNeil, and L. D. Clark, "Factors influencing the biocompatibility of insertable silicon microshafts in cerebral cortex," *IEEE Trans. Biomed. Eng.*, vol. 39, pp. 635–43, June 1992.
- [79] D. R. Kipke, D. S. Pellinen, and P. J. Rousche, "CNS recording electrodes and techniques," in *Neuroprosthetics: Theory and Practice*, K. Horch and G. S. Dhillon, Eds. London, U.K.: Imperial College Press, 2003.
- [80] V. Braitenberg and A. Schuz, *Cortex: Statistics and Geometry of Neuronal Connectivity*. New York: Springer-Verlag, 1998.
- [81] D. R. Humphrey and W. S. Corrie, "Properties of the pyramidal tract neuron system within a functionally defined subregion of primate motor cortex," *J. Neurophysiol.*, vol. 41, pp. 216–243, 1978.
- [82] D. R. Humphrey and E. M. Schmidt, "Extracellular single-unit recording methods," in *Neurophysiological Techniques: Applications to Neural Systems*, A. A. Boulton, Ed. Totowa, NJ: Humana, 1990.
- [83] J. N. Turner, W. Shain, D. H. Szarowski, M. Andersen, S. Martins, M. Isaacson, and H. Craighead, "Cerebral astrocyte response to micromachined silicon implants," *Exp. Neurol.*, vol. 156, pp. 33–49, 1999.
- [84] W. Shain, L. Spataro, J. Dilgen, K. Haverstick, S. Retterer, M. Isaacson, M. Saltzman, and J. N. Turner, "Controlling cellular reactive responses around neural prosthetic devices using peripheral and local intervention strategies," *IEEE Trans. Neural Syst. Rehab. Eng.*, 2003, to be published.
- [85] J. W. Fawcett and R. A. Asher, "The glial scar and central nervous system repair," *Brain Res. Bull.*, vol. 49, pp. 377–391, 1999.
- [86] J. D. Kralik, D. F. Dimitrov, D. J. Krupa, D. B. Katz, D. Cohen, and M. A. Nicolelis, "Techniques for long-term multisite neuronal ensemble recordings in behaving animals," *Methods*, vol. 25, pp. 121–150, 2001.
- [87] X. Cui, V. A. Lee, Y. Raphael, J. A. Wiler, J. F. Hetke, D. J. Anderson, and D. C. Martin, "Surface modification of neural recording electrodes with conducting polymer/biomolecule blends," *J. Biomed. Mater. Res.*, vol. 56, no. 2, pp. 261–72, 2001.
- [88] A. Branner and R. A. Normann, "A multielectrode array for intracortical recording and stimulation in sciatic nerve of cats," *Brain Res. Bull.*, vol. 51, pp. 293–306, 2000.
- [89] P. K. Campbell, R. A. Normann, K. W. Horch, and S. S. Stensaas, "A chronic intracortical electrode array: Preliminary results," *J. Biomed. Mater. Res.*, vol. 23, pp. 245–59, 1989.
- [90] E. M. Maynard, C. T. Nordhausen, and R. A. Normann, "The Utah intracortical electrode array: A recording structure for potential brain-computer interfaces," *Electroencephal. Clin. Neurophysiol.*, vol. 102, pp. 228–239, 1997.
- [91] C. T. Nordhausen, E. M. Maynard, and R. A. Normann, "Single-unit recording capabilities of a 100 microelectrode array," *Brain Res.*, vol. 726, pp. 129–140, 1996.
- [92] R. A. Normann, D. J. Warren, J. Ammermuller, E. Fernandez, and S. Guillory, "High-resolution spatio-temporal mapping of visual pathways using multi-electrode arrays," *Vision Res.*, vol. 41, pp. 1261–1275, 2001.
- [93] P. J. Rousche and R. A. Normann, "Chronic recording capability of the Utah intracortical electrode array in cat sensory cortex," *J. Neurosci. Methods*, vol. 82, pp. 1–15, 1998.
- [94] J. Csicsvari, B. Jamieson, K. D. Wise, and G. Buzsaki, "Mechanisms of gamma oscillations in the hippocampus of the behaving rat," *Neuron*, vol. 37, pp. 311–322, Jan. 2003.
- [95] J. Csicsvari, D. A. Henze, B. Jamieson, K. D. Harris, A. Sirota, P. Barthó, K. D. Wise, and G. Buzsáki, "Massively parallel recording of unit and local field potentials with silicon-based electrodes," *J. Neurophysiol.*, vol. 90, pp. 1314–1323, June 2003.
- [96] J. G. Arenberg, S. Furukawa, and J. C. Middlebrooks, "Auditory cortical images of tones and noise bands," *JARO*, vol. 1, pp. 183–194, 2000.
- [97] J. Perez-Orive, O. Mazar, G. C. Turner, S. Cassenaer, R. I. Wilson, and G. Laurent, "Oscillations and sparsening of odor representations in the mushroom body," *Science*, vol. 297, pp. 359–365, 2002.
- [98] Y.-X. Fu, K. Djupsund, H. Gao, B. Hayden, K. Shen, and Y. Dan, "Temporal specificity in the cortical plasticity of visual space representation," *Science*, vol. 296, pp. 1999–2003, 2002.
- [99] H. A. Swadlow, A. G. Gusev, and T. Bezdudnaya, "Activation of a cortical column by a thalamocortical impulse," *J. Neurosci.*, vol. 22, pp. 7766–7773, 2002.
- [100] S. M. Brierer and D. J. Anderson, "Multi-channel spike detection and sorting using an array processing technique," *Neurocomputing*, vol. 26, pp. 947–956, 1999.
- [101] D. R. Kipke, R. J. Vetter, J. C. Williams, and J. F. Hetke, "Silicon-substrate intracortical microelectrode arrays for long-term recording of neuronal spike activity in cerebral cortex," *IEEE Trans. Neural Syst. Rehab. Eng.*, 2003, to be published.
- [102] X. Cui, V. A. Lee, Y. Raphael, J. A. Wiler, J. F. Hetke, D. J. Anderson, and D. C. Martin, "Surface modification of neural recording electrodes with conducting polymer/biomolecule blends," *J. Biomed. Mater. Res.*, vol. 56, no. 2, pp. 261–272, 2001.
- [103] D. H. Szarowski, M. D. Andersen, S. Retterer, A. J. Spence, M. Isaacson, H. G. Craighead, J. N. Turner, and W. Shain, "Brain responses to micromachined silicon devices," *Brain Res.*, 2003, to be published.
- [104] R. H. Olsson III, M. N. Gulari, and K. D. Wise, "Silicon neural recording arrays with on-chip electronics for in-vivo data acquisition," in *Proc. IEEE-EMBS Int. Conf. Microtechnology Medicine and Biology*, 2002, pp. 237–240.



- [105] —, "A fully-integrated bandpass amplifier for extracellular neural recording," in *Proc. 1st IEEE/EMBS Int. Conf. Neural Engineering*, 2003, pp. 165–168.
- [106] Y. Yao, M. N. Gulari, J. F. Hetke, and K. D. Wise, "A self-testing multiplexed CMOS stimulating probe for a 1024-site neural prosthesis," in *Proc. IEEE Int. Conf. Solid-State Sensors, Actuators, and Microsystems (Transducers '03)*, pp. 1213–1216.
- [107] H. Yu and K. Najafi, "Low-power interface circuits for bio-implantable microsystems," presented at the Int. IEEE Solid-State Circuits Conf. (ISSCC) 2003, San Francisco, CA.
- [108] M. Ghovanloo, K. D. Wise, and K. Najafi, "Toward a button-sized 1024-site wireless cortical microstimulating array," in *Proc. 1st Int. IEEE/EMBS Conf. Neural Engineering*, 2003, pp. 138–141.
- [109] M. Ghovanloo and K. Najafi, "A fully-digital frequency-shift-keying demodulator chip for wireless biomedical implants," in *Proc. IEEE Southwest Symp. Mixed-Signal Design (SSMSD 2003)*, pp. 223–227.
- [110] F. C. Flack, E. D. James, and D. M. Schlapp, "Mutual inductance of air-cored coils: Effect on design or radio frequency coupled implants," *Med. Biol. Eng.*, vol. 9, pp. 79–85, 1971.
- [111] W. H. Ko, S. P. Liang, and C. D. Fung, "Design of radio-frequency powered coils for implant instruments," *Med. Biol. Eng. Comp.*, vol. 15, pp. 634–640, 1977.
- [112] M. Soma, D. G. Galbraith, and R. L. White, "Radio-frequency coils in implantable devices: Misalignment analysis and design procedure," *IEEE Trans. Biomed. Eng.*, vol. BME-34, pp. 276–282, Apr. 1987.
- [113] D. G. Galbraith, M. Soma, and R. L. White, "A wide-band efficient inductive transdermal power and data link with coupling insensitive gain," *IEEE Trans. Biomed. Eng.*, vol. BME-34, pp. 265–275, Apr. 1987.
- [114] W. J. Heetderks, "RF powering of millimeter and submillimeter-sized neural prosthetic implants," *IEEE Trans. Biomed. Eng.*, vol. 35, pp. 323–327, May 1988.
- [115] M. R. Shah, R. P. Phillips, and R. A. Normann, "A study of printed spiral coils for neuroprosthetic transcranial telemetry applications," *IEEE Trans. Biomed. Eng.*, vol. 45, pp. 867–876, July 1998.
- [116] C. R. Neagu, H. V. Jansen, A. Smith, J. G. E. Gardeniers, and M. C. Elwanspoek, "Characterization of a planar microcoil for implantable microsystems," *Sens. Actuators A*, vol. 62, pp. 599–611, 1997.
- [117] E. S. Hochmair, "System optimization for improved accuracy in transcutaneous signal and power transmission," *IEEE Trans. Biomed. Eng.*, vol. BME-31, no. 2, pp. 177–186, Feb. 1984.
- [118] C. M. Zierhofer and E. S. Hochmair, "High-efficiency coupling-insensitive transcutaneous power and data transmission via an inductive link," *IEEE Trans. Biomed. Eng.*, vol. 37, no. 7, pp. 716–722, July 1990.
- [119] —, "Geometric approach for coupling enhancement of magnetically coupled coils," *IEEE Trans. Biomed. Eng.*, vol. 43, no. 7, pp. 708–714, July 1996.
- [120] —, "The class-E concept for efficient wide-band coupling-insensitive transdermal power and data transfer," in *Proc. IEEE 14th EMBS Conf.*, vol. 2, 1992, pp. 382–383.
- [121] H. McDermott, "An advanced multiple channel cochlear implant," *IEEE Trans. Biomed. Eng.*, vol. 36, no. 7, pp. 789–797, July 1989.
- [122] —, "A custom-designed receiver-stimulator chip for an advanced multiple-channel hearing prosthesis," *IEEE J. Solid-State Circuits*, vol. 26, pp. 1161–1164, Aug. 1991.
- [123] B. Smith, P. H. Peckham, M. W. Keith, and D. D. Roscoe, "An externally powered, multichannel, implantable stimulator for versatile control of paralyzed muscle," *IEEE Trans. Biomed. Eng.*, vol. BME-34, no. 7, pp. 499–508, July 1987.
- [124] T. Akin, K. Najafi, and R. M. Bradley, "A wireless implantable multichannel digital neural recording system for a micromachined sieve electrode," *IEEE J. Solid-State Circuits*, pp. 109–118, Jan. 1998.
- [125] P. Mohseni and K. Najafi, "A wireless FM microsystem for biomedical neural recording applications," in *Proc. IEEE Southwest Symp. Mixed-Signal Design*, 2003, pp. 217–222.
- [126] Z. Tang, B. Smith, J. H. Schild, and P. H. Peckham, "Data transmission from an implantable biotelemetry by load-shift keying using circuit configuration modulator," *IEEE Trans. Biomed. Eng.*, vol. 42, pp. 524–528, May 1995.
- [127] M. Ghovanloo, K. Beach, K. D. Wise, and K. Najafi, "A BiCMOS wireless interface chip for micromachined stimulating microprobes," *Proc. IEEE-EMBS Special Topic Conf. Microtechnologies Medicine and Biology*, pp. 277–282, 2002.



**Kensall D. Wise** received the B.S.E.E. degree with highest distinction from Purdue University, West Lafayette, IN, in 1963 and the M.S. and Ph.D. degrees in electrical engineering from Stanford University, Stanford, CA, in 1964 and 1969, respectively.

From 1963 to 1965 (on leave 1965–1969) and from 1972 to 1974, he was a Member of Technical Staff at Bell Telephone Laboratories, where his work was concerned with the exploratory development of integrated electronics for use in telephone communications. From 1965 to 1972, he was a Research Assistant and then a Research Associate and Lecturer in the Department of Electrical Engineering at Stanford University, working on the development of integrated circuit technology and its application to solid-state sensors. In 1974, he joined the Department of Electrical Engineering and Computer Science at the University of Michigan, Ann Arbor, where he is now the J. Reid and Polly Anderson Professor of Manufacturing Technology and Director of the NSF Engineering Research Center for Wireless Integrated MicroSystems. His present research interests focus on the development of integrated microsystems for health care, process control, and environmental monitoring.

Dr. Wise organized and served as the first chairman of the Technical Subcommittee on Solid-State Sensors of the IEEE Electron Devices Society (EDS). He was General Chairman of the 1984 IEEE Solid-State Sensor Conference, Technical Program Chairman of the IEEE International Conference on Solid-State Sensors and Actuators (1985), and IEEE-EDS National Lecturer (1986). He served as General Chairman of the 1997 IEEE International Conference on Solid-State Sensors and Actuators. Dr. Wise received the Paul Rappaport Award from the EDS (1990), a Distinguished Faculty Achievement Award from the University of Michigan (1995), the Columbus Prize from the Christopher Columbus Fellowship Foundation (1996), the SRC Aristotle Award (1997), and the 1999 IEEE Solid-State Circuits Field Award. In 2002 he was named the William Gould Dow Distinguished University Professor at the University of Michigan. He is a Fellow of the AIMBE and a Member of the U.S. National Academy of Engineering.



**David J. Anderson** received the B.S.E.E. degree from Rensselaer Polytechnic Institute, Troy, NY, in 1961 and the M.S. and Ph.D. degrees from the University of Wisconsin, Madison, in 1963 and 1968, respectively.

After completing a postdoctoral traineeship with the Laboratory of Neurophysiology, University of Wisconsin Medical School, he joined the University of Michigan, Ann Arbor, where he is now professor of Electrical Engineering and Computer Science, Biomedical Engineering,

Biomedical Engineering and Otolaryngology.

Dr. Anderson is a Fellow of the American Institute for Medical and Biological Engineering, a member of the IEEE Neuroscience Society, the Acoustical Society of America, the Association for Research in Otolaryngology, and the Barany Society.



**Jamille F. Hetke** received the B.S.E.E. degree from Michigan State University, East Lansing, in 1985 and the M.S. degree in bioengineering from the University of Michigan, Ann Arbor, in 1987.

She has been involved in neural probe research at the University of Michigan since the completion of her degrees and is currently an Assistant Research Scientist in the Department of Electrical Engineering and Computer Science. She participates in research in the Kresge Hearing Research Institute and the Neural Engineering Laboratory, and is the main contact for investigators interested in obtaining probes from the Center for Neural Communication Technology. Her research interests are centered on the design of silicon arrays and implantable systems for eventual use in neuroprostheses.



**Daryl R. Kipke** (Member, IEEE) received the B.Sc. degree in engineering science, the M.Sc. degree in bioengineering, the M.S.E. degree in electrical engineering, and the Ph.D. degree in bioengineering from the University of Michigan, Ann Arbor, in 1985, 1986, 1988, and 1991, respectively.

From 1991 to 1992, he was a Research Associate in the Department of Bioengineering and the Institute for Sensory Research at Syracuse University, Syracuse, NY. In 1992, he was appointed

Assistant Professor in Bioengineering at Arizona State University, Tempe, where his research was focused in auditory neurophysiology, computational neuroscience, neuroprostheses, and bioMEMS. In 1998, he was promoted to Associate Professor in Bioengineering. In 2001, he joined the faculty of the College of Engineering at the University of Michigan to continue his work in bioMEMS for neural implants, neuroprostheses and brain-machine interfaces, systems neuroscience, and functional neurosurgery. He is currently an Associate Professor in the Departments of Biomedical Engineering and Electrical Engineering and Computer Science, University of Michigan, and the Director of the Neural Engineering Laboratory.



**Khalil Najafi** (Fellow, IEEE) was born in 1958. He received the B.S., M.S., and Ph.D. degrees in electrical engineering from the Department of Electrical Engineering and Computer Science, University of Michigan, Ann Arbor, in 1980, 1981, and 1986 respectively.

Since 1986, he has been with the Department of Electrical Engineering and Computer Science, University of Michigan. From 1986 to 1988 he was a Research Fellow; from 1988 to 1990, he was an Assistant Research Scientist; from 1990

to 1993, he was an Assistant Professor; from 1993 to 1998 he was an Associate Professor; since September 1998, he has been a Professor and the Director of the Solid-State Electronics Laboratory. He is an Associate Editor for the *Journal of Micromechanics and Microengineering* and an Editor for the *Journal of Sensors and Materials*. His research interests include micromachining technologies, solid-state micromachined sensors, actuators, and MEMS; analog integrated circuits; implantable biomedical microsystems; hermetic micropackaging; and low-power wireless sensing/actuating systems.

Dr. Najafi was awarded a National Science Foundation Young Investigator Award from 1992 to 1997. He was the recipient of the Beatrice Winner Award for Editorial Excellence at the 1986 International Solid-State Circuits Conference, the Paul Rappaport Award for coauthoring the Best Paper published in the IEEE Transactions on Electron Devices, and the Best Paper Award at ISSCC 1999. In 2001 he received the Faculty Recognition Award, and in 1994 the University of Michigan's Henry Russel Award for outstanding achievement and scholarship, and was selected as the Professor of the Year in 1993. In 1998, he was named the Arthur F. Thurnau Professor for outstanding contributions to teaching and research, and received the College of Engineering's Research Excellence Award. He has been active in the field of solid-state sensors and actuators for more than 18 years, and has been involved in several conferences and workshops dealing with solid-state sensors and actuators, including the International Conference on Solid-State Sensors and Actuators, the Hilton-Head Solid-State Sensors and Actuators Workshop, and the IEEE/ASME Micro Electromechanical Systems (MEMS) Conference. He is the Editor for solid-state sensors for IEEE TRANSACTIONS ON ELECTRON DEVICES and an Associate Editor for IEEE JOURNAL OF SOLID-STATE CIRCUITS.